CHARACTERIZATION OF ASTROCYTE AND OXYTOCIN NEURON ACTIVITY DYNAMICS IN THE PARAVENTRICULAR NUCLEUS OF THE HYPOTHALAMUS

JOSHUA JOHN RYCHLIK

CHARACTERIZATION OF ASTROCYTE AND OXYTOCIN NEURON ACTIVITY DYNAMICS IN THE PARAVENTRICULAR NUCLEUS OF THE HYPOTHALAMUS

By JOSHUA RYCHLIK, B.Sc

A Thesis Submitted to the School of Graduate Studies in Fulfilment of the Requirements for the Degree Master Sciences

McMaster University MASTER OF NEUROSCIENCE (2022) Hamilton, Ontario

TITLE: **CHARACTERIZATION OF ASTROCYTE AND OXYTOCIN NEURON ACTIVITY DYNAMICS IN THE PARAVENTRICULAR NUCLEUS OF THE HYPOTHALAMUS**

AUTHOR: Joshua Rychlik B.Sc. (McMaster University)

SUPERVISOR: Professor Katrina Choe

NUMBER OF PAGES: vii, 76

Lay Abstract

The goals of this thesis are to identify how two key cell types of the paraventricular nucleus of the hypothalamus (PVN), namely oxytocin (OXT) neurons, and astrocytes interact with each other during stress and social situations. We employed fiber photometry in mice to investigate the interactions between PVN astrocytes and OXT neurons during social and stress experiments. We found that PVN astrocytes are strongly activated during the stress response and immediately prior to sniffing a non-familiar mouse. On the other hand, we found that PVN OXT neurons did not elicit a response in our stress tests but did increase in activity during social sniffs. Interestingly, we also found that PVN OXT neurons reduce in activity while a mouse sniffs an almond odour. These results suggest that PVN astrocytes are active during stressful stimuli while PVN OXT neurons are active during periods of socialization and decrease in activity while sniffing an appetitive odour.

Abstract

The paraventricular nucleus of the hypothalamus (PVN) is at the axis of stress and social responses. During stress, PVN corticotropin-releasing hormone (CRH) neurons become active and release arginine vasopressin (AVP) and CRH onto downstream targets. While CRH and AVP initiate the release of glucocorticoids into the blood stream, AVP also binds to receptors on PVN astrocytes to induce calcium waves. Previous studies have found that PVN astrocyte activity is important for modulating CRH neuron activity. It has been shown that oxytocin (OXT), the social hormone, is also released in the PVN during stress to provide anxiolytic effects. We hypothesize that stress-induced OXT release in the PVN acts on PVN astrocyte receptors to provide the anxiolytic effects seen in previous studies. We sought to explore this hypothesis by using fiber-photometry on C57Bl/6 mice during a social odour preference test, freely behaving social tests, the looming shadow stress task, and the tail lift procedure. We found that PVN OXT neurons are active while a mouse sniffs another mouse and decrease in activity while a mouse sniffs an appetitive odour. We also found that PVN astrocytes are active during stressful tasks and are active moments before a mouse interacts with a non-familiar mouse. We did not see any interactions between these two cell types during our experiments. An experimental technique with a higher temporal resolution may be needed in the future to better identify if and how these two cell types interact to modulate PVN CRH neuron activity.

Acknowledgements

First and foremost, I would like to thank my supervisor Dr. Katrina Choe for allowing me the opportunity to complete my Masters degree within her lab, providing me with guidance and support, and allowing me to be part of the beginnings of a very productive lab.

I would also like to thank my parents for the love and support they have given me when I needed it the most. You have always supported me and my pursuits of interest.

To my lab mates, Katy, Aishwarya, Madeleine, Katherine, Gabrielle, and Manav for making the lab space a comfortable, friendly, and (most important of all) fun environment to work in and all the help you have given me throughout this project.

And a special thanks to Dave for continuously helping us move equipment to-and-fro, and for all the behind-the-scenes work he performs when creating lab experiment apparatus.

Contents

List of Tables and Figures

List of Abbreviations and Symbols

(ACTH) Adrenocorticotropic hormone

(AMY) Amygdala
- **(BLA)** Basolateral Amygdala
- **(CeA)** Central Amygdala
- **(MeA)** Medial Amygdala

(AVP) Arginine Vasopressin
- **(AVPr)** Arginine Vasopressin Receptor

(BNST) Bed Nucleus of Stria Terminalis

(BBB) Blood-Brain Barrier

(CPU) Caudate-putamen

(CNS) Central Nervous System

(CSF) Cerebrospinal fluid

(CC) Cingulate Cortex

(CRH) Corticotropin-releasing Hormone

(DRN) Doral Raphe Nucleus

(FDR) False-Discovery Rate

(GECI's) Genetically Encoded Calcium Indicators

(GPCRs) Guanine Protein-Coupled Receptors

(HPC) Hippocampus

(HPA) Hypothalamic-Adrenal-Pituitary

(i.p.) Intraperitoneal (Injection)

(LS) Lateral Septum

(LC) Locus Coeruleus

(MPOA) Medial Preoptic Area

(NAc) Nucleus Accumbens

(OXT) Oxytocin
- **(OXTr)** Oxytocin Receptor
- **(MagnOXT)** Magnocellular Oxytocin
- **(ParvOXT)** Parvocellular Oxytocin

(OVLT) Organum Vasculosum Laminae Terminalis

(PBN) Parabrachial Nucleus

(PVN) Paraventricular Nucleus of the Hypothalamus

(PAG) Periaqueductal Grey

(PP) Posterior Pituitary

(PFC) Prefrontal Cortex

(SN) Substantia Nigra

(SCN) Suprachiasmatic Nucleus

(SON) Supraoptic Nucleus

(VP) Ventral Pallidum

(VTA) Ventral Tegmental Area

(VMA) Ventromedial Nucleus of the Hypothalamus

Declaration of Academic Achievement

This thesis is organized in a regular (non-sandwich) thesis format. The thesis consists of four sections. Section 1 is a literature review of the important stress and social cells within the paraventricular nucleus of the hypothalamus and an introduction to the experiments performed for the rest of the thesis. Section 2 outlines the methods underlying the experiments performed. Section 3 shows the results and important findings of our experiments. Section 4 is a discussion on our findings, including future areas of research based on our findings.

The majority of the work on the experiments was performed by me with the aid of lab members as outlined here. Katy Celina Sandoval aided in perfusions, slicing after behavioural experiments, scoring behaviour data via Boris software and post-hoc confocal microscopy imaging. Madeleine Matthews and Katherine Andrec aided in scoring behavioural data via Boris software. Aishwarya Patwardhan aided in post-hoc confocal microscopy imaging.

1.The characterization of the stress response within the paraventricular nucleus of the hypothalamus

1.1 Introduction to stress

Stress research began as early as 1915 by Walter Bradfort Cannon as he observed the bodily changes that occurred after various external stimuli, such as cold, hunger, pain, exercise, and strong emotional stimuli (Godoy et al., 2018). These early studies into the stress response allowed Canon to coin the term "*Fight-or-flight"* to describe the response taken by an individual undergoing stress to mitigate further stressors. Stress research was then built upon by Hans Seyle, who discovered a "General Adaptive Syndrome", a three-stage event of common symptoms which occurs after exposure to various acute nocuous agents such as exposure to extreme cold, surgical injury, excessive exercise, or intoxications to various nonlethal drugs (Seyle, 1976). The symptoms noticed by Seyle and other early stress researchers were believed to be responses that return the body to homeostasis after disruption, such as increasing glucose to replenish lost energy stores, inhibiting T-cell proliferation to reduce inflammation, and decreasing the activity of non-stress related hormones (such as reproductive related hormones, or bone and muscle growth hormones) to decrease energy expenditure (Herman et al., 2003). These findings had been expanded to be defined as "the active process of adapting and maintaining homeostasis through the production of mediators such as cortisol" caused by psychosocial, physiological/metabolic, or traumatic stimuli (McEwen & Akil, 2020). Early findings on the stress response are what led to research related to the Hypothalamic-Pituitary-

Adrenal (HPA) axis and the deep underpinnings of the stress response. The HPA axis is a neurohormone feedback system between the central nervous system (CNS) and the adrenal glands and is an important mediator for the stress response (Spencer & Deak, 2017). The HPA axis will be discussed further in section 1.2.

After the identification of the HPA axis, researchers discovered that there are many neuropeptides and hormones responsible for modulating the stress response for future events. Although corticotropin-releasing hormone (CRH) is a main player in the stress response in the paraventricular nucleus of the hypothalamus (PVN), other neurohormones such as arginine vasopressin (AVP) and oxytocin (OXT) play important roles in modulating CRH release and subsequent stress responses (Zelena et al., 2015; Smith et al., 2016). More recently, it has been found that local astrocytes play a larger role than previously believed in stress response modulation as well (Section 1.5.1). This review will identify these key players in the PVN, these stress cells' roles, their connections to other brain regions, and how they relate to the stress response itself, while providing a basis for future studies.

1.2 The HPA Axis

Psychological and physiological stress begins by activation of the HPA axis by the release of CRH. CRH is a 41 amino acid peptide that is synthesized within CRH neurons of the PVN and acts upon two types of guanine protein-coupled receptors (GPCRs): CRHr1 and CRHr2 (Dautzenberg & Hauger, 2002; Joelz & Baram, 2009). Before understanding how PVN stress cells can be modulated, one must understand

the HPA axis, and the stress response at its most basic level (Figure 1). Stress can be categorized into two domains: psychological stress, and physiological or homeostatic challenges. Psychological stress such as work stress, relationship stress, or financial stress initiates a response in the prefrontal cortex (PFC), amygdala, and hippocampus before reaching the bed nucleus stria terminalis (BNST) (Bains et al., 2015). Neurons from the BNST then synapse onto the PVN to allow for CRH production and release. On the other hand, physiological or homeostatic challenge stress such as infection, temperature stress, or pain begin at various nuclei within the brainstem such as the raphe nuclei, parabrachial nucleus, locus coeruleus, and nucleus of the solitary tract (Lipositz et al., 1987; Myers et al., 2017). Various neurons from these brainstem nuclei then synapse onto the PVN, although some homeostatic challenges will cause activation of brainstem to PFC, amygdala, and/or hippocampus activation before synapsing with the BNST, similar to the psychological stress circuitry (Figure 1; Herman et al., 2002; Herman et al., 2005; Roland & Sawchenko, 1993; Review: Bains et al., 2015). GABA and/or glutamate activation from the BNST and/or brainstem stimulates CRH neurons within the PVN which finally leads to CRH and AVP mobilization and release into the hypothalamus to begin the activation of the HPA axis (Plotsky, 1985; Review: Kovacs, 2013). CRH binds to CRHr1 receptors within the pituitary gland to cause a surge of adrenocorticotropic hormone (ACTH) release which will then travel through systemic circulation to bind to the adrenal cortex above the kidneys (Bains et al., 2015). Once ACTH reaches the adrenal cortex, ACTH will enact the release of glucocorticoids into the peripheral blood stream. Glucocorticoids are endogenous steroids that are often used as a stress marker and act upon many different cell types to

enact a large number of changes within cells to redirect bodily energy for a suitable stress response (Herman et al., 2016). To regulate further stress responses, glucocorticoids will eventually make their way back up to the PVN by crossing the blood-brain barrier (BBB) and bind to glucocorticoid receptors on CRH neurons to inhibit further activity and reduce further CRH release (Erkut et al., 1998; Herman et al., 2016).

An Interesting study performed by Daviu et al. (2020) sought to better understand CRH neuron activity using fiber photometry during the looming shadow stress test. Fiber photometry is a technique where a fiber optic cannula is implanted into a brain area of interest alongside a viral vector containing genetically-encoded calcium indicators (GECI's) to visualize the activity levels of cell populations during *in vivo* recordings (Gunaydin et al., 2014). In the looming shadow stress test, a mouse is placed within a home cage with a small house that the mouse is previously habituated to. A computer monitor is then placed on top of the home cage while the mouse is allowed to freely roam the cage. After a baseline fiber photometry recording, a small (2 cm) black shadow appears on the monitor briefly, then expands to 20 cm to stay in a looming state for several seconds (Münch, 2013; Daviu et al., 2020). This test is used to replicate a predator flying from above and elicits a fear response in the experiment mouse. The experiment mouse then responds in one of three ways: the mouse will run under the house for safety, freeze in place, or show no behavioural response. Daviu et al. found that PVN CRH neurons increase in activity during the looming shadow stimulus. Daviu et al. then furthered this finding and showed that there is a small increase in CRH neuron activity ~2 seconds prior to the large increase in CRH neuron activity during

initiation of “run” behaviour, but not other types of behaviours. Based on these results, the authors concluded that CRH neurons show a unique increase in activity prior to behaviour initiation in controllable, but not uncontrollable stress, and this may be important for stress-related decision making. It is therefore important to note that stress-related decision making may begin at the PVN and involve local circuitry before creating downstream effects for stress behaviour initiation.

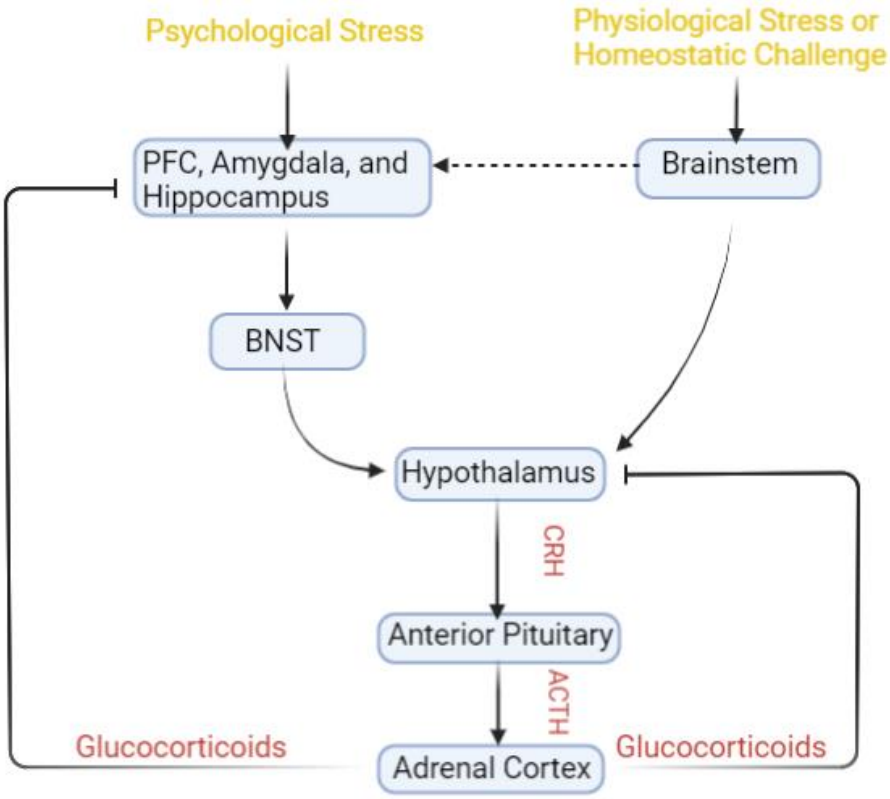

Figure 1. HPA-Axis Activation following Psychological and Physiological Stress or Homeostatic Challenge. Psychological stress begins with activation of the prefrontal cortex (PFC), amygdala, and hippocampus before activating the bed nucleus of stria terminalis (BNST). This leads to activation of the hypothalamus before corticotropin-releasing hormone (CRH) is released into the anterior pituitary and adrenocorticotropic hormone (ACTH) is released into the adrenal cortex. Finally, glucocorticoids are released by the adrenal cortex which offers a negative feedback to the PFC, amygdala and hippocampus, and hypothalamus to reduce further CRH release. Physiological stress or homeostatic challenge offers a similar pathway but begins at the brainstem before activating the PFC, amygdala and hippocampus, or directly to the hypothalamus. (Adapted from Bains et al., 2015).

1.3 Neurohypophyseal Nonapeptides

The next two key players in the PVN for the stress response are AVP and OXT. In 1955 Vincent du Vigneaud won the Nobel prize for synthesizing and describing the nature of both AVP and OXT (Vigneaud et al., 1954a; Vigneaud et al., 1954b). During this time, it was believed that these two nonapeptides of similar structure were produced in the posterior pituitary, but it wasn't until 1964 that Sachs and Takabatake were able to show that they are produced in the hypothalamus before being transported to the posterior pituitary for secretion into peripheral circulation (Sachs et al., 1968; Review: Rotondo et al., 2016). Neurohypophysial hormones contain a disulphide bridge at residues 1 and 6 which results in a six-amino acid cyclic structure with a 3 amino acid residue tail (Figure 2). The amino acid at position 3 and 8 defines whether the hormone is OXT, or AVP; in OXT, position 3 is the amino acid isoleucine, and position 8 is leucine while AVP contains phenylalanine at position 3 and arginine at position 8 (Gimpl & Farhenholz, 2001).

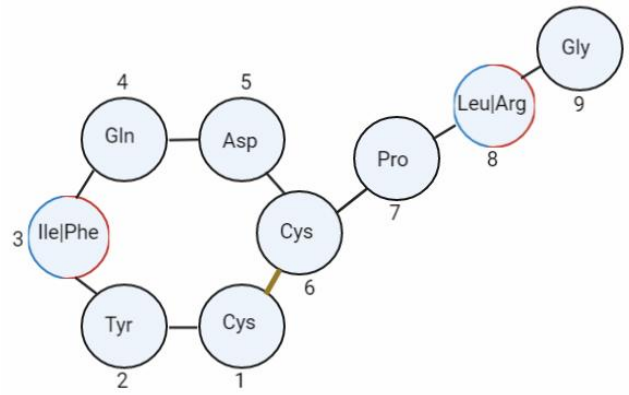

Figure 2. A Depiction of Neurohypophysial Nonapeptides showing the six-amino acid cyclic structure with a 3 amino acid tail. Isoleucine (Ile) in slot 3 and leucine (leu) in slow 8 would depict oxytocin, while phenylalanine (Phe) in slot 3 and arginine (Arg) in slot 8 would depict arginine vasopressin. A disulphide bridge (yellow) between cysteine (Cys) residues in slot 1 and 6 are in both nonapeptides. Numbers denote amino acid number within nonapeptide (Adapted from Song & Albers, 2018).

AVP has well established roles in fluid homeostasis by regulating water absorption and vasoconstriction while OXT is known as the 'love hormone' for its importance with lactation, parturition, and prosocial behaviours (Grantham & Burg, 1966; Creager et al., 1986; Soloff et al., 1979; Nishimora et al., 1996; Ross & Young, 2009; Bartz et al., 2011). Interestingly, both neuropeptides are implicated in socialization. A study by Lim & Young (2004) employed the use of V_{1A} receptor (an AVP receptor) antagonists and c-fos expression to identify that V_{1A} receptors in the ventral pallidum are necessary for pair-bond formation in monogamous prairie voles. The roles OXT plays in socialization will be discussed in greater detail in section 1.4. OXT has been found to have opposing effects in terms of anxiety and depression and therein striking a strong balance in activity between these two homologous neuropeptides is important for protection against these pathologies (Neumann & Landgraf 2012). How these two neuropeptides affect the stress response may also act as opposing forces. An interesting study by Windle et al., 2004 compared the effects of AVP and OXT in rats undergoing restraint stress for 30 minutes and found that rats intracerebroventrically injected with OXT had reduced levels of ACTH mobilization and reduced corticosteroids in the bloodstream, while AVP had no effects on these variables (Windle et al., 2004). Although this observation suggests that AVP may not have an effect in attenuating the stress response during restraint stress, other studies have indicated that AVP does indeed have an importance in the stress response.

A study performed by Rivier & Vale, 1983 set out to understand the relationship between AVP and stress by measuring plasma ACTH levels pre-, and post-ether vapour

exposure (a well-established physiological stress trigger). Rivier & Vale injected rats intravenously with saline or an AVP antagonist (dPTyr(Me)AVP) before subjecting them to 3 minutes of ether stress before decapitation at either 10 minutes, or 20 minutes post ether vapour exposure. Rivier & Vale had found that the AVP antagonist decreased blood plasma ACTH levels in the 20 minute post-stress rats, but not the 10 minutes post-stress mice, indicating that AVP is important for late periods of stress activation (Rivier & Vale, 1983). A further study by Abou-Samra et al. in 1987 had used cultured anterior pituitary cells from Sprague-Dawley rats to discover that infusion with AVP alone does not affect ACTH release, but instead acts alongside CRH by stimulating adenylate cyclase activity (generates cAMP) and inhibiting phosphodiesterase (degrades cAMP) (Abou-Samra et al., 1987). This finding highlights how AVP acts in conjunction with CRH to increase the “gain” in the stress response once CRH binds to cells in the pituitary, and this explains why we would see AVP antagonists effect ACTH release in a chronic stressed state, rather than acute. These findings were followed up with studies on chronic stress in adults. Studies by de Goeij et al., 1991 and Makino et al., 1995 reveal that in adult rats there is an increase in AVP-expressing CRH neurons, while the number of CRH neurons themselves remain unchanged (de Goeij et al., 1991; Makino et al., 1995). The belief is that in adult chronic stress paradigms, CRH neurons in the PVN increase the amount of AVP available for mobilization to increase stress reactivity to a wider range of potential stressors (Aguilera at al., 2008). This increased stress reactivity, or hyper-reactivity, could be debilitating if there was no other neuropeptide to oppose AVP’s synergistic effects. Thankfully, we have a yin to AVP’s yang within the PVN to oppose this.

1.4 Oxytocin

OXT is an evolutionarily preserved neurohypophysial nonapeptide hormone created within the PVN, supraoptic nucleus (SON), and the accessory nuclei of the hypothalamus (Jurek & Neumann, 2018). Once synthesized into large-dense core vesicles within OXT neurons, OXT is then transported to neurohypophysial terminals and the dendrites of OXT neurons. Upon stimulation by either vaginocervical distension during birth, suckling during lactation, sexual stimulation, various forms of stress, or socialization, these large-dense core OXT vesicles release OXT from axon terminals and/or from the soma and dendrites of PVN and SON OXT neurons (De Jong et al., 2015; Ebner et al., 2005; Ivell, 1986; Neumann, 2009; Steinman et al., 2016; Van Tol et al., 1988; Van Tol., 1987; Wotjak et al., 2001). OXT is then released peripherally into the bloodstream by posterior pituitary projecting neurons and secreted into cerebrospinal fluid (CSF), and/or secreted into specific brain areas for central OXT release (Jurek & Neumann 2018). Recent preliminary findings by Perkinson et al. in 2021 used fiber photometry to visualize large bursts of PVN OXT neuron activity during mouse lactation. Through further investigation, Perkinson et al. noticed smaller bursts of activity prior to mouse lactation events. Perkinson et al. hypothesize that these small bursts prime somato-dendritic OXT release and are necessary to create the large, coordinated PVN OXT bursts required for lactation in mice (Perkinson et al., 2021). Although this study is currently ongoing, these preliminary findings highlight important OXT neuron activity dynamics that can be seen when recording populations of PVN OXT neurons using fiber photometry.

In addition to its physiological roles, OXT has been established to play an important role in social behaviour. According to current literature, the central secretion of OXT is believed to act as a social salience cue to prime the brain for social interactions, including social reward (Anpilov et al., 2020; Tang et al., 2020; Review: Jurek & Neumann, 2018). Resendez et al. (2020) recently used *in* vivo two-photon microscopy coupled with GECI's in male mice to visualize the activity levels of OXT neurons during social encounters. They identified that 52% of visualized OXT neurons were active while the test mouse was exposed to a juvenile male mouse, while 32% of visualized OXT neurons were active during a non-social stimulus (empty plastic bottle). This finding not only identifies the importance of OXT neurons for pro-social behaviours, but also emphasizes the importance of understanding specific subpopulations of PVN OXT neurons which will be discussed further in sections 1.4.2 and 1.4.3.

1.4.1 The Oxytocin Receptor

The OXT receptor (OXTr) is a 7 trans-membrane domain G protein-coupled receptor (GPCR) that can be found peripherally in the uterus, kidney, ovaries, testis, thymus, heart, vascular endothelium, osteoclasts, and myoblasts to enact various body-wide effects such as milk ejection and parturition in mothers (Gimpl and Fahrenholz, 2001; Zingg and Laporte, 2003). In the murine brain, OXTrs have been found to be expressed in the central, medial, and basolateral amygdala (CeA, MeA, BLA, respectively), nucleus accumbens (NAc), bed nucleus of stria terminalis (BNST), PVN, medial preoptic area (MPOA), ventromedial nucleus of the hypothalamus (VMA), hippocampus (HPC), ventral pallidum, PAG, striatum, lateral septum (LS), ventral

tegmental area (VTA), and olfactory bulb (Figure 3; Dabrowka et al., 2011; Hiroaka, 2016; Shaprio & Insel, 1989; Review: Grinevich et al., 2015). Interestingly, OXTr expression has been found to vary depending on whether an animal is monogamous or polygamous in nature, for example: monogamous prairie (Microtus ochrogaster) and pine (Microtus pinetorum) voles show significant levels of OXTR in the NAc, but the closely related polygamous montane (Microtus montanus) and meadow (Microtus pennsylvanicus) voles have much lower receptor density in this area (Insel and Shapiro, 1992; Ross et al., 2009). This gives us insight on the specific functions OXTr's have with pro-social behaviours and how OXTr expression in the NAc can affect these behaviours.

Although understanding where OXTr's are located and manipulating OXTr function is useful for understanding how behaviour can be affected, this approach only allows investigation of its function at the gross level. More recent studies have investigated OXT neuronal projections to brain areas to better identify exact electrical and morphological effects on downstream neurons that can affect brain area development and behaviour. PVN OXT neurons are canonically divided into 2 categories based on their shape, size, localization, physiology, and projections: Parvocellular OXT (parvOXT) neurons, and magnocellular OXT (magnOXT) neurons. Previous studies have revealed that these two cell types are found at an approximate 3:1, magnOXT to parvOXT neuron ratio within the murine PVN (Lewis et al., 2020; Chen et al., 2022). Further details on these two canonical groups of OXT neurons will be discussed in the below sections 1.4.2 and 1.4.3.

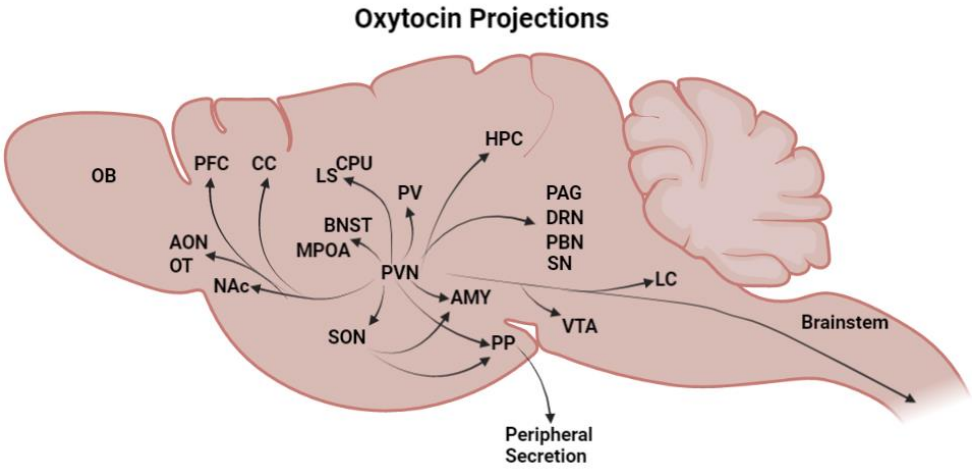

Figure 3. Oxytocin Neural Network Diagram in Rodents. A depiction highlighting PVN OXT neuron projections in the rodent brain. Amygdala (AMY), Bed nucleus of the stria terminalis (BNST), Caudate-putamen (CPU), Cingulate Cortex(CC), Dorsal raphe Nucleus (DRN), Hippocampus (HPC), Lateral septum (LS), Locus Coeruleus (LC), Medial Preoptic Area (MPOA), Nucleus Accumbens (NAc), Olfactory Bulb (OB), Olfactory Tubercle (OT), Organum vasculosum laminae teriminalis (OVLT), Parabrachial nucleus (PBN), Posterior Pituitary (PP), Paraventricular nucleus (PVN), Periaqueductal Grey (PAG), Periventricular Nucleus hypothalamus (PV), Prefrontal cortex (PFC), Substantia Nigra (SN), Suprachiasmatic Nucleus (SCN), Supraoptic Nucleus (SON), Ventral Pallidum (VP), Ventral Tegmental Area (VTA) (Adapted from Song and Albers, 2018; Jurek & Neumann, 2018).

1.4.2 Magnocellular Oxytocin Neurons

MagnOXT neurons are relatively large in size (20-30 μm) and primarily project to the posterior pituitary to enact widespread peripheral action by releasing OXT into the bloodstream (Althammer & Grinevich, 2017). One feature that separates magnOXT neurons from parvOXT neurons are the smaller amplitude (64.2±1.1 mV) and longer duration (1.1±0.1 ms) spikes, with an A-type transient outward potassium current that appears as a ‘shoulder’ in electrophysiological traces (Tasker & Dudek, 1991). This electrophysiological phenomenon is believed to increase the duration of action potential firing to allow for a longer release of OXT into the peripheral blood stream and CSF

(Tasker & Dudek, 1991). This allows for the widespread and slow actions of magnOXT. A recent study by Zhang et al., 2021 used a dual-retrograde tracing and 3D reconstruction of the rat neurohypophysial system to better understand magnOXT projections within the brain. Zhang et al. found that not only did magnOXT neurons project to the posterior pituitary, but a proportion of these cells also formed collateral connections to the amygdala, caudate putamen, and the NAc for CNS alterations. These findings are supported by previous literature that had found that magnOXT neurons project to the CeA for fear response and aggression, the caudate/putamen for locomotion and social exploration, and the NAc for social reward (Knobloch et al., 2012; Calcagnoli et al., 2014; Althammer & Grinvevich 2017).

1.4.3 Parvocellular Oxytocin Neurons

ParvOXT neurons have smaller cell bodies (~10-20 μm) and are localized more caudally within the PVN (Althammer & Grinevich, 2017). ParvOXT neurons can also be identified by their electrical properties, where ParvOXT neurons have T-type calcium currents which allows these cells to have a large (66.5±1.6 mV) but shorter (0.9±0.1 ms) spiking behaviour (Tasker and Dudek, 1991). As opposed to magnOXT, ParvOXT are known to terminate at the spinal cord and brainstem to modulate vital physiological and autonomic functions, such as: regulating food intake, breathing, copulation, cardiovascular reactions, gastric reflexes, and pain perception (For Review: Althammer & Grinevich, 2017; Swanson et al., 1980; Wrobel et al., 2009; Blevins et al., 2004; Mack et al., 2002; Sabatier et al., 2013; Rash et al., 2014; Juif et al., 2013). Other studies have shown that parvOXT neurons also project to many other CNS brain areas

including the NAc, VTA, substantia nigra (SN), and magnOXT neurons within the SON (Lewis et al,. 2020; Xiao et al., 2013). An interesting study by Tang et al., 2020 investigated parvOXT neuron's role for social touch in female rats by visualizing increased c-fos expression and increased calcium activity through fiber photometry in parvOXT neurons after a non-nociceptive touch. This finding was followed up using retrograde tracers to identify parvOXT projections onto magnOXT neurons before using chemogenetics to activate or inhibit these parvOXT neurons. Tang et al. had found that activation of these parvOXT neurons increases social touch behaviour while inhibition decreases social touch, and anogenital sniffing behaviours (Tang et al., 2020). These findings not only highlight the importance of parvOXT neurons for prosocial behaviours but also identify an important step in communication for peripheral OXT release.

1.4.4 Oxytocin in the stress response

Early studies on the PVN had found that not only is CRH released during a stress response, but OXT is as well. A study by Lang et al. in 1983 had found that the forced swim test or restraint stress increased blood plasma OXT and AVP levels, while cold stress did not. This finding was furthered by Nishioka et al. in 1998 who employed an *in vivo* microdialysis in the PVN of rats and found that shaker stress (a stress test where rats are placed within a plastic cylinder atop of a shaking platform at 110 cycles/min for 10 minutes) induced a large increase in OXT within the PVN, but not outside of the PVN. A number of other stressors, such as foot shock, social defeat stress, and noise stress were used to confirm the results that OXT is a stress hormone, in some way (de Jong et al., 2015, Engelmann et al., 2001; Windle et al., 1997; Wotjak et al., 2001).

Interestingly, about 40% of magnOXT neurons also express CRH, while no parvOXT have shown to have this feature (Dabrowska et al., 2013). A study by Windle et al. (1997) first gave a hint of a potential anxiolytic role for OXT in the stress response. Windle et al. administered OXT or saline intracerebroventricularly during a noise stress test and found that rats given OXT had a reduced plasma corticosterone concentration, reduced rearing behaviour and increased open-arm entries in an elevated-plus maze - an indication of reduced anxiety-like behaviours. These findings were furthered by Nomura et al. (2003) who measured a marked increase in PVN CRH mRNA following restraint-stress in OXT KO mice, more so than wildtype mice. This gives the hint that during stress, PVN OXT is also being released and used in some way to decrease PVN CRH mediated stress response. A study by Smith and Wang in 2014 examined a potential interaction between stress-induced OXT release and social pair-bonding of prairie voles, giving us a unique perspective on stress and OXT dynamics. They found that monogamous female prairie voles showed reduced anxiety-like behaviour and plasma corticosterone levels after restraint stress if their male partner was present during recovery, as opposed to social isolation. These results potentially suggest that having a familiar partner present may increase OXT release which then aids in dampening the stress response. Finally, recent pharmacological studies have found that OXT is able to dampen the stress response by acting upon GABA-A receptors on PVN CRH neurons to reduce CRH activity (Smith et al., 2016; Pati et al., 2020). Although pharmacological studies are useful for identifying how a substrate could affect specific brain area processes, there is no way of determining the intricate pathways involved and more importantly, if there are any interneurons or mediators involved. In the next

section (1.5) we will discuss astrocytes as a possible mediator of anxiolytic effects by OXT and how this mediator has been found to be important for the AVP and CRH systems in the PVN.

1.5 Astrocytes

Astrocytes are a classic part of the tripartite synapse that provide a netting around neurons to remove and recycle excess neurotransmitters from one synapse and to reduce neurotransmitter diffusion to nearby synapses (Weber & Barros, 2015). In 1990, researchers surprisingly found that astrocytes can also become excited during this process, and this leads to calcium waves within the astrocyte (Cornell-Bell et al., 1990; Review: Hamilton & Atwell, 2010). These calcium waves within astrocytes can be localized to subdomains of astrocyte branches or even pass through electrical synapses, called gap junctions, to connected astrocyte arbours to activate even more astrocytes (Giaume et al., 2010). Astrocytes then have the ability to release 'gliotransmitters' to enact various changes to nearby neurons, such as long-term potentiation, long-term depression, and neuronal pruning (Parpura et al., 1994; Nedergaard, 1994; Henneberger et al., 2010; Chen et al., 2013; Review: Faust et al., 2021). This allows the astrocyte to be a large contributor to alterations in region-wide signal transduction and an important component in neuronal activity.

1.5.1 Astrocytes in Stress

As astrocytes are a key player in many, if not all, synapses, it is unsurprising that PVN astrocytes play a role in the stress response. A recent study by Chen et al. in 2019 has found that upon CRH neuron activation, PVN astrocytes are activated by concurrent AVP release (Figure 4). In turn, calcium waves within PVN astrocytes allow astrocyte-astrocyte activation and the release of ATP to nearby neurons. This ATP then binds to GABA and glutamate neurons to modulate CRH neuron activity by a local feedback mechanism. This interesting mechanism leads to the ability for large scale modulation of PVN circuitry via local glutamate and GABA synapses. Although these findings showcased that PVN astrocyte activation is important for CRH neuron modulation via AVP mobilization, we still do not know how OXT fits into this picture. A recent study by Wahis et al. in 2021 sought to understand whether OXT neurons from the PVN are able to alter amygdalar astrocyte activity levels. Wahis et al. employed viral tracing and optogenetics to discover that PVN OXT neurons project to, and activate, CeA astrocytes. These CeA astrocytes then expel D-serine to nearby interneurons to increase NMDA transmission and ultimately inhibit output projection neurons, resulting in anxiolysis (Wahis et al., 2021). A similar mechanism involving astrocytes could occur within the PVN to activate GABA local circuits to reduce CRH release into the pituitary. Indeed, *in vitro* studies have reported that PVN astrocytes do express OXTrs and that application of OXT induces calcium wave activity in these astrocytes (Mittaud et al., 2001; Di-Scala Guenot & Strosser, 1998). Therefore, it is possible that AVP is not the only neurohypophyseal nonapeptide that is able to modulate CRH neuron activity via astrocyte activation.

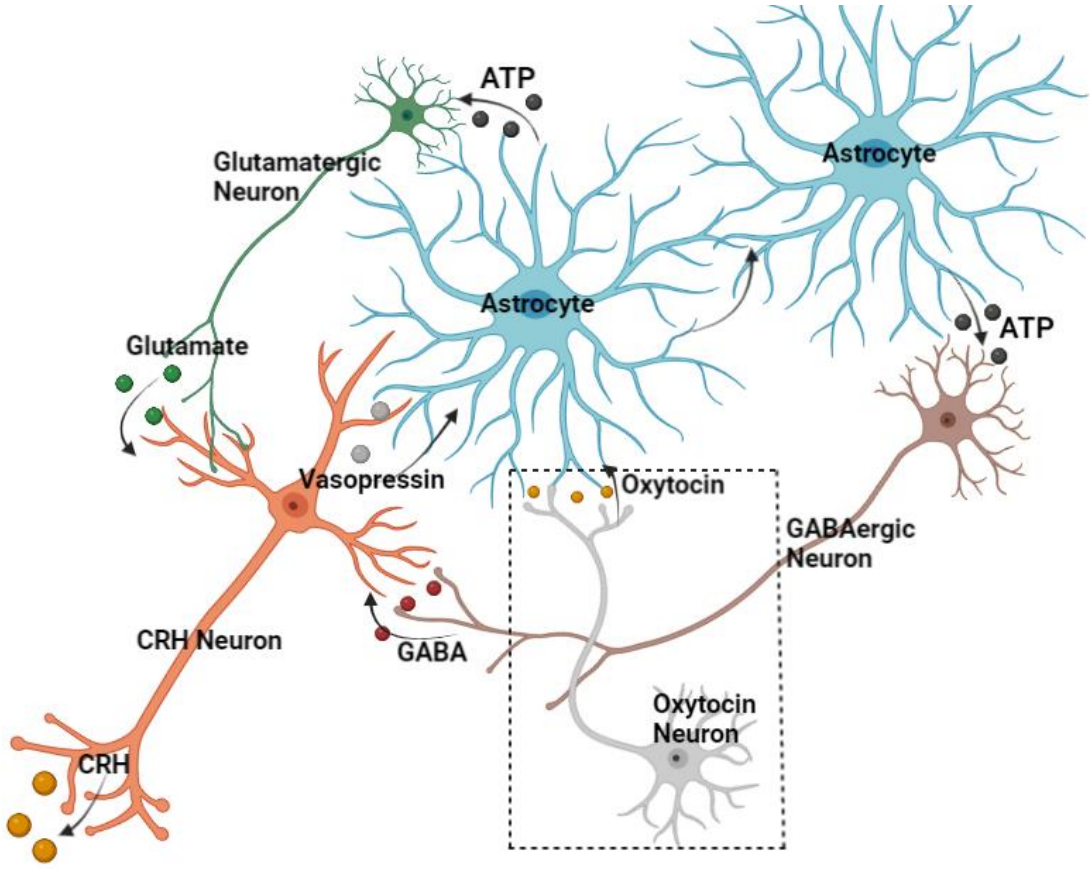

Figure 4. Diagram showing local PVN astrocyte interactions with CRH neurons. Norepinephrine released during stress activated CRH neurons which release CRH and AVP. AVP then binds to local astrocytes which release ATP onto GABA and/or glutamate neurons which feedback onto CRH neurons to modulate activity levels (Adapted from Chen et al., 2019). Dotted box shows the current hypothesis where stress causes a release of oxytocin onto PVN astrocytes to further modulate the CRH activity via astrocyte activity.

1.6 Conclusion

To summarize thus far, CRH, AVP, OXT, and PVN astrocytes in the PVN all participate in the stress response. CRH has its widely known negative feedback mechanism via glucocorticoids released from the adrenal cortex, yet it also has a lesser-known local feedback mechanism that can control the stress response before even reaching the pituitary for ACTH release. During a stress response AVP is released

alongside CRH to act as a “gain” in the pituitary and increase ACTH release by acting locally on PVN astrocytes to release ATP onto nearby GABAergic and/or glutamatergic neurons (Abou-Samra et al. 1987; Chen et al., 2020). The molecular and cellular mechanism by which OXT is able to affect GABA-A receptors on PVN CRH neurons to reduce CRH release is presently unknown. Therefore, we hypothesize that during stress, PVN OXT neurons are activated and somatically release OXT onto nearby astrocytes to modulate future CRH release through a similar mechanism of AVP-induced astrocyte activity (Figure 4). To experimentally test this hypothesis, we employed fiber photometry to simultaneously visualize calcium activity within astrocytes and OXT neurons in the PVN. We subjected mice to a social odour preference test, freely-behaving social tests, and looming shadow and tail lift stress tasks. This allowed us to identify real time astrocyte and OXT cell activity during social and stressful simulations that are likely to activate 1 or both cell types. We have found that PVN astrocytes do not alter in activity while a mouse sniffs a social, or non-social (almond) odour. PVN OXT neurons were also unaltered as a mouse sniffed a social odour but interestingly, decreased in activity while a mouse sniffed the non-social (almond) odour. During freely-behaving social tests, PVN astrocytes increased in activity moments before sniffing a non-familiar juvenile conspecific but did not change while sniffing a familiar conspecific, in contrast to this, PVN OXT neurons increased in activity while a mouse sniffed a familiar, or non-familiar mouse. Finally, we found that PVN astrocytes increase in activity during the looming shadow and tail lift stress tasks, while PVN OXT neurons did not change in activity.

2. Methods

Table 1.

Metadata of mice used in behavioural data analysis. (X shows if data used in analysis)

Cohort	Name	Sex	Date of Birth (DD-MM-YY)	Date of Surgery (DD-MM-YY)	Age at time of Surgery (days)	Genotype	Single or Dual Channel	Odour Test	Social Test	Looming Shadow	Tail Lift
4	A90	M	10-03-21	25-06-21	111	WT	Single	X	X	X	
4	A91	M	10-03-21	25-06-21	111	WT	Single	X	X	X	
6	B74	M	03-05-21	24-07-21	82	WT	Single	X	X	X	
8	C20	M	25-05-21	07-08-21	74	WT	Single	X	X	X	
8	C42	F	06-06-21	07-08-21	62	WT	Single	X	Low Sniff Behaviour	X	
16	G40	M	14-02-21	01-04-22	46	WT	Single	X	X	X	
16	G41	M	14-02-21	01-04-22	46	WT	Single	X	X	X	
16	G42	M	14-02-21	01-04-22	46	WT	Single	X	X	X	
16	F62	F	22-11-21	31-03-22	129	Oxt-Cre	Dual	Corrupt	Low Sniff Behaviour	X	X
15	F66	F	22-11-21	11-02-22	81	Oxt-Cre	Dual	X	X	X	X
15	F67	F	22-11-21	11-02-22	81	Oxt-Cre	Dual	X	X	X	X
15	F69	F	22-11-21	11-02-22	81	Oxt-Cre	Dual	X	X	X	X
15	F71	M	22-11-21	10-02-22	80	Oxt-Cre	Dual	X	X	X	X
15	F72	M	22-11-21	10-02-22	80	Oxt-Cre	Dual	X	X	X	X
16	F79	M	22-11-21	31-03-22	129	Oxt-Cre	Dual	X	X	Corrupt	Corrupt
17	H25	M	01-03-22	20-05-22	80	Oxt-Cre	Dual	To be scored	To be scored	X	X
17	H30	F	01-03-22	20-05-22	80	Oxt-Cre	Dual	To be scored	To be scored	X	X
17	H33	F	01-03-22	20-05-22	80	Oxt-Cre	Dual	To be scored	To be scored	X	X

2.1 Experimental Animals

C57BL/6 mice are known for their identical genetics due to a high degree of inbreeding which allows for a reduction in variation between individual mice. Adult (11 weeks old) C57BL/6 mice were used as test mice for these experiments. Oxt-Cre C57BL/6 mice were used for AAV2/9-EF1a-DIO-RCaMP2 injections to allow Cre-induced expression of RCaMP2 in PVN OXT cells. After stereotaxic surgery the mice were allowed to recover for 3 weeks before beginning behaviour testing protocols. All procedures were performed as outlined in the Choe lab Animal Use Protocol (AUP 20-12-45) approved by the McMaster University Animal Research Ethics Board (AREB). Individual mouse metadata are listed in Table 1.

2.2 Stereotaxic Fiber Implantation and Injection

Wildtype c57Bl/6 male and female mice were used for single-channel astrocyte fiber photometry recordings. To achieve cell-specific dual-channel recordings of PVN OXT cells, male and female Oxt-Cre C57Bl/6 mice were used. Stereotaxic surgery was performed while the mice were under isoflourane anesthetic to target the right side PVN (A/P -0.56, L/M +0.2, D/V -4.8 mm) and 0.5ml of AAV2/5-promGFAP-GCAMP6f (single-channel recordings), or 0.6 ml of an equal mixture of AAV2/5-promGFAP-GCAMP6f and AAV2/9-EF1a-DIO-RCaMP2 (dual-channel recordings) was injected at a rate of 0.02 ml per minute and allowed to diffuse for 5 minutes before the needle was withdrawn. An implantable 0.48 NA, 400 µm fiber optic cannula (Doric Lenses) was implanted to target the right PVN (A/P -0.56, L/M +0.2, D/V -4.8 mm). Mice were injected with 5 mg/kg

carprofen for 3 days post-surgery and allowed for 3 weeks to recover before beginning experimental tests.

2.3 Fiber Photometry Recording and Analysis

Fiber photometry recordings in freely behaving mice were recorded using the Doric fiber photometry system. Fiber Photometry allows for the recording of calcium transient signals, by use of GECI's, in freely behaving mice. Fluorescent signal data were retrieved at a 1 kHz sampling rate with two (single-channel), or three (dual-channel) excitatory LEDs. A 405 nm isosbestic and a 480 nm (GCaMP6) excitatory LED were used in all recordings, while a 570 nm (RCaMP2) excitatory LED was used only in dual-channel recordings. Prior to behaviour testing the intensity of each LED was recorded to be between 10 – 15 mW (isosbestic), or 30-50 mW (GCaMP6, RCaMP2) as this range allows for excitation of GECI's with limited photo-bleaching. After GECI excitation, an emittance light was received by the 6-port Doric minicube to disentangle retrieved light.

Signal data were then exported to Matlab (Mathworks) for offline data analysis using FPA-Analysis Tool (L.A. Molina, 2021, unpublished). Each signal was individually fit with a second-order polynomial curve before subtraction to remove any artifacts due to photobleaching. The isosbestic signal was then aligned to each excitatory signal using a least-squares linear fit. Finally, the change in fluorescence (ΔF) was calculated by subtracting the 405 nm isosbestic signal from each of the 480 nm and 570 nm excitatory signals at each time point. Z-score was further calculated by the following equation: $z = (F - F0)/\sigma F$, where F is the test signal, $F0$ and σF are the mean and

standard deviation of the basal signal, respectively (Guo et al., 2015). A low-pass filter of 0.3 Hz was applied to each signal to better interpret data retrieved.

Video recordings were time-locked to fiber photometry recordings at a rate of 16 frames-per-second. Video recordings were analyzed using Boris software by two blinded experimenters. Two specific epoch criteria were enacted to remove any irregular data points: Baseline irregularity, and Epochs within 5 seconds of each other. Baseline irregularity is defined by a clear indication that the baseline recording was not steady. Any epochs within 5 seconds of each other were also deleted as they would show extraneous spikes during the baseline, or would have a reduced expression of signal due to cell kinetics.

For trace recordings, the z-score for each animal's trials were uploaded to excel. The mean during the baseline (-8s to –3s for odour and social tests; -5 to 0 for looming shadow, -10 to –5 for tail lift) was subtracted for each individual mouse trial. Then the mean and SEM of all the trials were calculated and plotted on GraphPad.

For line graphs, bins were taken and averaged at each time point depicted before being plotted on GraphPad with SEM.

For heatmaps, each individual trial for each mouse was extracted and placed on excel. Each timepoint within each individual trial was normalized to the baseline using the formula☹Timepoint1-MininumBaselineValue)/(MinimumBaselineValue-MaximumBaselineValue). This allowed the visualization of peaks and troughs as they occur within 0 to 1 normalized values. These values were then plotted as heatmaps using GraphPad.

2.4 Behaviour Experiments

All mice (test mice and stimulatory mice) were handled for 3-5 minutes for 3 days (with 1 rest day in between) prior to the start of behavioural testing to allow for mouse-to-experimenter habituation. Each mouse was subjected to a 1-hour habituation period in minimal light prior to each behaviour test. During mouse habituation and behaviour testing, a white noise machine was used to reduce any extraneous noise. A Honeywell air filter was also used to remove any accumulation of odours and mouse dander. The following behavioural protocol was used for each mouse: Day 1: Open-Field Test (OFT) and Odour Test, Day 2: Rest Day, Day 3: Social 1, Day 4: Rest Day, Day 5 Social 2, Day 6 Rest Day, Day 7 Social 3, Day 8 to 12 Looming Shadow Habituation, Day 13 Looming Shadow Test. Tail lift data was acquired during Social 2 and Social 3 experiments as mice were placed in the center cage (Section 2.4.2).

2.4.1 Odour Tests.

7 male and 1 female C57-Bl/6 mice were used for single-channel recordings, while 3 male and 3 female mice were used for dual-channel recordings for odour tests. To reduce photo-bleaching which may occur over long periods of GECI excitation, the LED excitation light was turned off during the open-field test. This allowed experimental mice to become acclimatized to the fiber optic cable while exploring an open field arena (25.7 cm X 25.7 cm X 30 cm). After 20 minutes of OFT testing, the LED's were turned on and a 5 minute baseline recording commenced. A cotton swab was either dipped in 1:100 diluted almond extract or run through a same-sex unfamiliar mouse cage (as per

Yang and Crawley, 2009) to serve as a non-social or social odour. At t=5 minutes, the 2 cotton swabs were placed at opposite sides of the open field arena. The test mouse was allowed to freely explore the two cotton swabs while a video recording and Doric software simultaneously captured mouse movement and calcium transients.

2.4.2 Social Tests.

For social tests, there was 7 male mice for single-channel recordings, and 3 male and 3 female mice for dual-channel recordings. 1 week prior to behavioural testing a same-sex wildtype C57BL/6 mouse (aged 4-6 weeks) was placed in the home cage of the test mouse to allow for familiarization between mice. Same-sex wildtype C57BL/6 mice aged 4-6 weeks were also selected and used as unfamiliar stimulatory mice. This juvenile age group was chosen to reduce intermale aggression during testing day. Familiar and non-familiar social experiments were conducted using three home cages, side-by-side with an opaque wall around each to reduce mouse visibility outside of the testing area. Test mouse and stimulus mouse were placed in the distant home cages with one empty home cage in between for a 10 minute habituation period and baseline recording. After the habituation period, both mice were simultaneously placed into the center home cage to allow for a 10-minute socialization period. Sniffs greater than 1 second in length were used for experimental analysis. Mice with less than or equal to 3 (greater than 1 second) sniffs were excluded due to abnormally low sniffing behaviour.

2.4.3 Looming Shadow Test.

For the looming shadow test, 7 male and 1 female mice were recorded for single-channel recordings while 6 female and 3 male were recorded in dual-channel mode. Mice were placed in a homecage setting with a 21-inch LCD monitor placed on top, position facing downwards as outlined by Daviu et al., 2020. A small shelter was placed within the homecage (13 cm X 12 cm X 10 cm) to allow for mouse escape. Mice were habituated to the testing apparatus, including home cage for 5 consecutive days (10mins per day) prior to testing day. On the testing day the mouse was placed within the looming shadow apparatus and allowed to roam during a 10 minute baseline recording. After the initial 10 minutes the experimenter triggered the appearance of the looming shadow at (at least) 1 minute intervals where a 2 cm black disc would appear. After 3 s the black disc expanded to a total diameter of 20 cm (over 2 s) before looming for 3 more seconds for a total of 8 seconds. A total of 6 - 8 trials over a 10 minute period were completed for each mouse.

Mouse behaviour was scored based on whether the mouse ran, froze, or did not respond to the shadow. A run behaviour was determined if the mouse ran towards the shelter during the looming shadow appearance. A freeze behaviour was scored if the mouse did not appear to move (except for breathing). A no response behavior was scored if the mouse did not show a run, or a freeze behaviour. No response behaviours were removed from further data analysis.

2.4.4 Tail Lift Procedure

6 female and 3 male Oxt-Cre mice were placed in a solo home cage for 10 minutes while fiber photometry was being recorded. At the 10-minute mark mice were lifted by their tail for 2-3 seconds before being placed within a separate home cage. Mice were then scored offline using Boris software from the beginning of the tail lift until the end of the tail lift. Data was transferred to Excel for further analysis.

2.5 Post-hoc Confirmation

2.5.1 Perfusions

Mice were perfused within 3 weeks after the looming shadow test. Mice were weighed then injected (i.p.) with 0.05 ml of (1.33 g/kg) sodium pentobarbital (Euthanyl). After mice were anesthetized they were pinned at a 30 degree angle. A 5 cm vertical incision was made on the abdomen and two 2 cm horizontal incisions were made at the top of the vertical incision to allow the opening of the abdominal cavity. The diaphragm was then cut and the chest was opened to allow access to the heart. A small cut was made at the right atrium to allow the outflow of blood. 20 ml (1x) Phosphate-Buffered Saline (PBS, Sigma) solution was then injected into the left ventricle to perfuse the mouse of blood. 20 ml of 4% paraformaldehyde (PFA, FujiFilm) solution was then injected into the left ventricle to fix the brain. The mouse was then decapitated and the brain was removed and submerged in 4% PFA solution. The fixed brain was then kept in a dark fridge for at least 24 hours before sectioning and mounting.

2.5.2 Sectioning and Mounting

Prior to sectioning, brains were washed using (1x) PBS solution. Brains were then placed on a brain mold and a coronal section was made around the visual cortex. The brain was then dried using a paper towel before being glued to a vibratome stand. The brain was then submerged in an ice cold PBS solution. 50 μm sections were made throughout the PVN. Brain sections were then moved to a blank slide and sections were ordered from rostral to caudal position. 0.3ml of mounting medium (Fluoromount-G with DAPI, Invitrogen) was placed the sections before the slide was enclosed and left to dry.

2.6 Statistics

Traces and quantification results are represented as mean ± SEM. Statistical analysis was performed using GraphPad 6 software. Quantitative data statistics were completed using repeated measures two-way ANOVA with the two-stage linear step-up false-discovery rate (FDR) method by Benjamini, Krieger, and Yekutieli. Adjusted P-values (Q) less than 0.05 were considered significant.

3. Results

3.1 PVN Astrocytes do not respond to sniffing a social or non-social odour

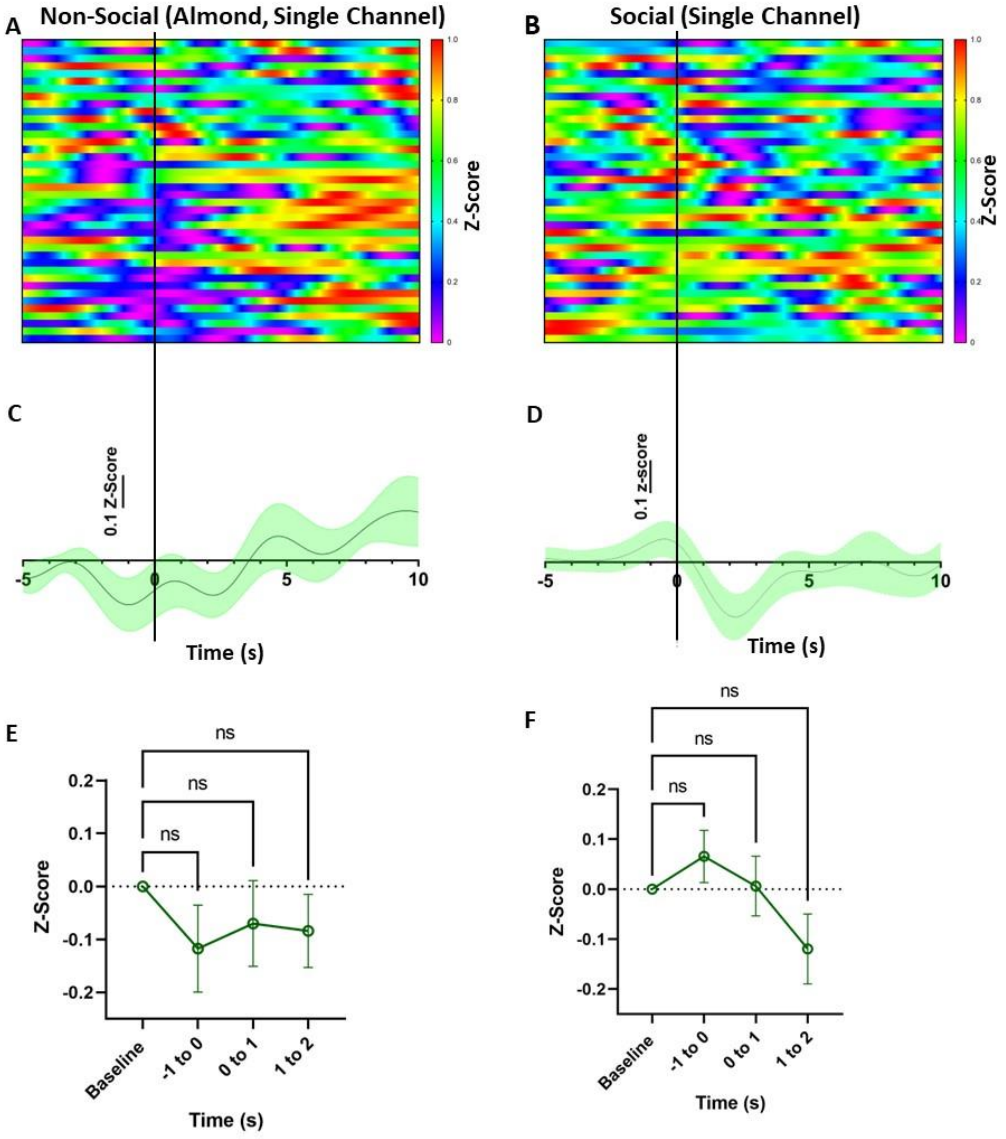

Figure 5. Calcium activity from PVN astrocytes during odour sniffing. (A, B) Heatmaps depicting changes in fluorescence of GFAP-GCaMP6 with non-social (almond) or social odour as recorded in single channel fiber photometry upon sniff onset (black vertical line). **(C, D)** Mean (green) traces of GFAP-GCaMP6f signal on onset of sniff (time = 0 s) with social or non-social odour (line [mean Z-score]; shade [SEM]). (**E, F)** Line graphs depicting 1 s average signal ± SEM. Two-way RM ANOVA, multiple comparisons test with FDR correction (ns denotes non-significance; n=40 trials, 8 mice).

To test whether PVN astrocytes respond to an odour of a non-familiar mouse, the population activity of PVN astrocytes were recorded using single-channel fiber photometry in 8 mice (40 trials). The PVN of 8 mice were injected with AAV-promGFAP-GCaMP6f viral load (0.6ml) and implanted with a fiber optic cannula. After 3 weeks of recovery the mice were allowed to freely behave in an open-field chamber with a social and a non-social (almond) scent at either end of the chamber. There were no significant changes in GCaMP fluorescence while mice were sniffing the non-social odour (Figure 1. A, C, E). The large standard error of mean suggests that there is a degree of variability in changes of fluorescence activity between mice while sniffing the nonsocial odour. While mice sniffed the social odour there was a slight (non-significant) increase in GCaMP fluorescence at the -1 to 0 second time period, and a slight (non-significant) decrease at the 1 to 2 second time period (Figure 1. C). These findings suggest that a social odour alone does not elicit a significant alteration in PVN astrocyte calcium wave activity, or that PVN astrocytes do not alter in activity from a social or non-social odour.

3.2 PVN Astrocytes and OXT neuron activity changes during odour sniffing

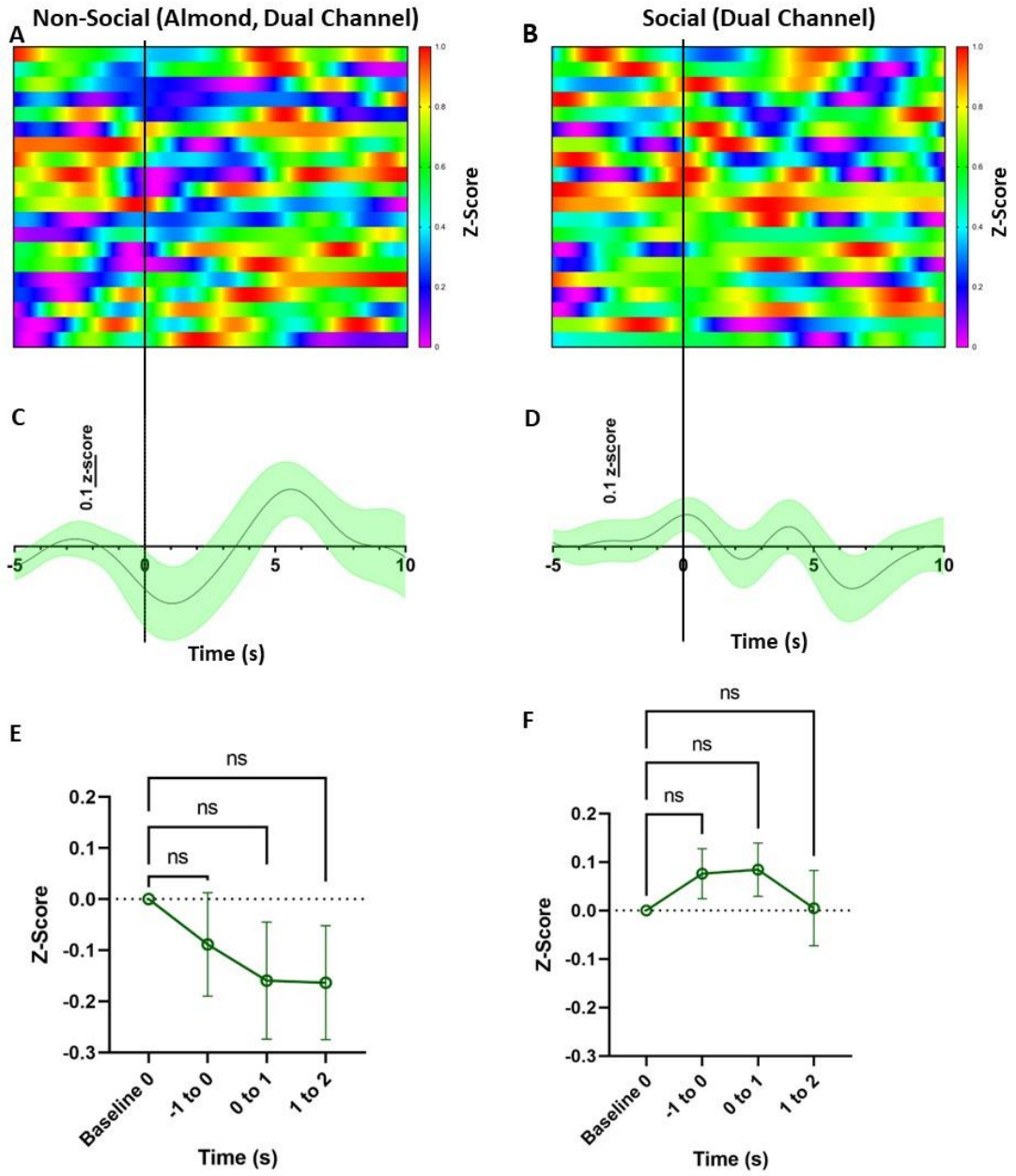

Figure 6. Calcium activity from PVN astrocytes during odour sniffing in dual-channel recordings. A,B Heatmaps showing average changes in fluorescence of GFAP-GCaMP6 in dual-channel fiber photometry upon sniff onset (black vertical line) of social or non-social (almond) odour **(C, D)** Mean (green) traces of GFAP-GCaMP6f signal on onset of sniff (time = 0 s with social or non-social odour) (line [mean Z-score]; shade [SEM]). (**E, F)** Line graphs depicting 1 s average signal ± SEM. Two-way RM ANOVA, multiple comparisons test with FDR correction (ns denotes non-significance; n=20 trials, 6 mice).

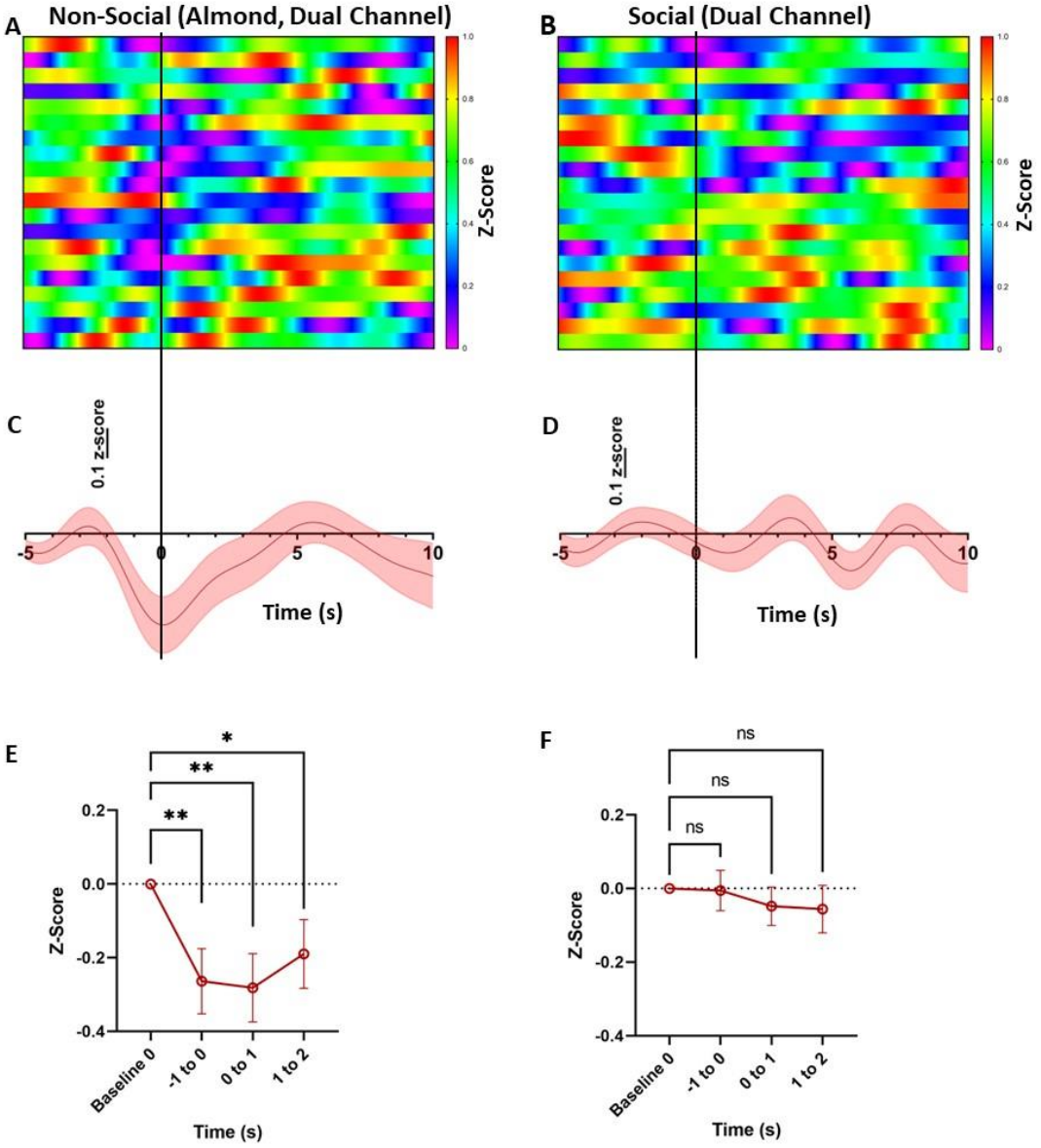

Figure 7. Calcium activity from PVN oxytocin neurons during odour sniffing in dual-channel recordings. A,B Heatmaps showing average changes in fluorescence of GFAP-GCaMP6 in dual-channel fiber photometry upon sniffing onset (black vertical line) of social or non-social (almond) odour. **(C, D)** Mean (red) traces of GFAP-GcaMP6f signal on onset of sniff (time = 0 s) with social or non-social odour (line [mean Z-score]; shade [SEM]). (**E, F)** Line graphs depicting 1 s average signal ± SEM. Two-way RM ANOVA, multiple comparisons test with FDR correction (ns denotes non-significance; * denotes Q<0.05, ** denotes Q < 0.01; n=20 trials, 6 mice).

Odour tests were repeated in 6 Oxt-Cre mice with injections of the same AAV-promGFAP-GCaMP6f virus and with the addition of AAV-EF1a-DIO-RCaMP2 virus (n=20 trials). This combination of viral load was mixed at a 1:1 ratio and allowed for the visualization of calcium activity within PVN OXT alongside PVN astrocytes in a dual-channel fiber photometry configuration. In GCaMP6 recordings there was no significant alteration seen in calcium fluorescence during social, or non-social (almond) odour sniffing (Figure 6). These findings replicated what we have previously seen in single-channel recordings (Figure 5) and provide further evidence that PVN astrocytes do not respond to social or non-social scents alone. In RCaMP2 recordings it was found that the scent of a same-sex conspecific did not alter PVN OXT neuron activity (Figure 7. B, D, E). Interestingly, as mice sniffed the non-social (almond) scent there was a significant decrease in RcaMP2 signal (Figure 7. A, C, E). This decrease in fluorescence began at least 1 second before the sniff occurred (mean z-score -0.2639; Q = 0.004), as the mouse approaches the scent. This decrease persisted up to 2 seconds after the sniff was initiated (Figure 7 C, E; mean z-score 0.1899; Q=0.0078). These findings indicate that the population of recorded PVN OXT neurons do not change in activity during sniffing a social odour alone, and these cells may require a stronger social stimulus to become active. In contrast to this, an appetitive (almond) scent significantly decreases PVN OXT neuron activity.

3.3 PVN astrocyte activity increases prior to social sniff with a non-familiar mouse

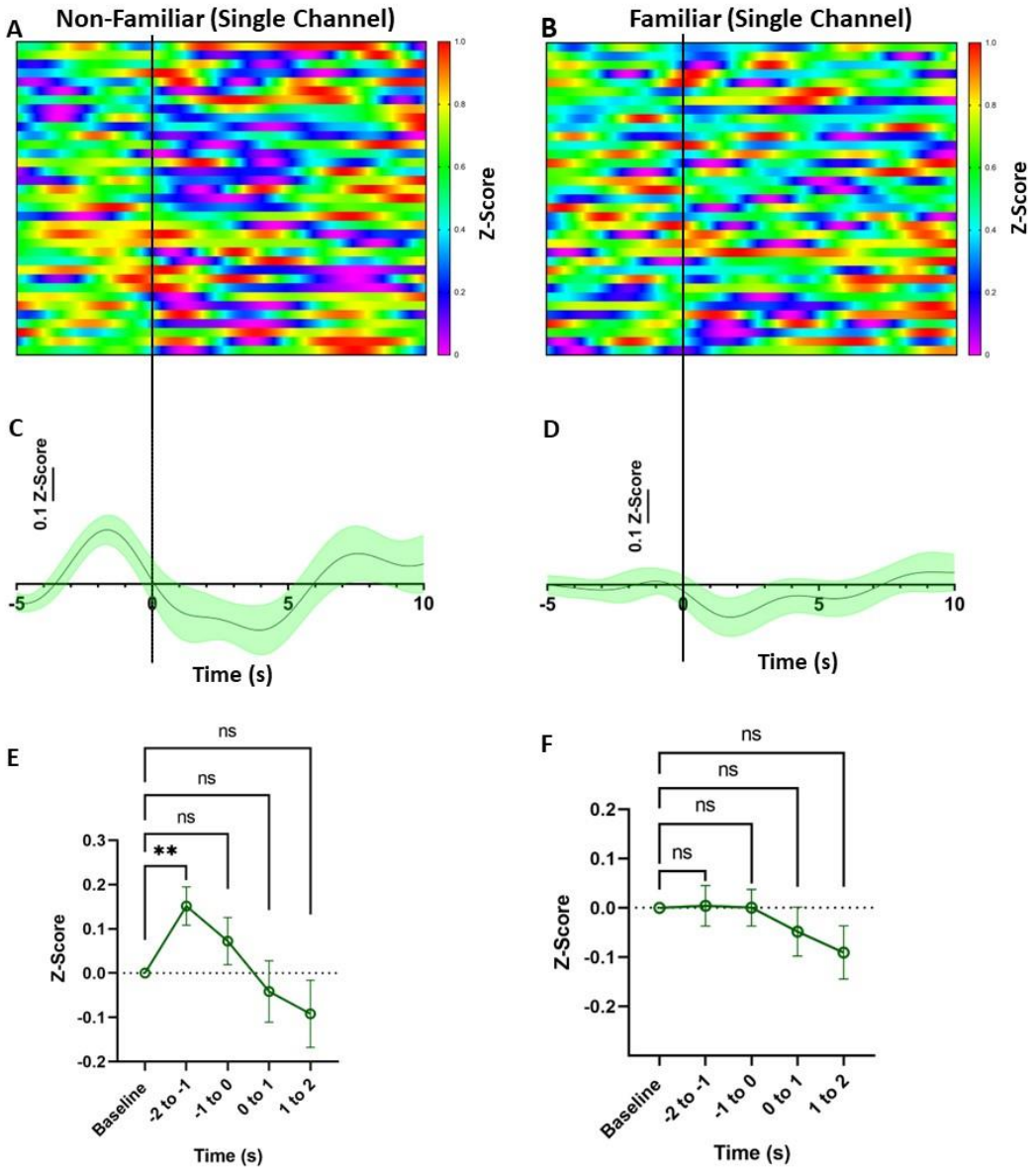

Figure 8. Calcium activity from PVN astrocytes during social sniffing in single-channel recordings. A,B Heatmaps depicting average changes in fluorescence of GFAP-GCaMP6 in single-channel fiber photometry upon sniffing onset (black vertical line) of familiar or non-familiar conspecific **(C, D)** Mean (green) traces of GFAP-GCaMP6f signal on onset of sniff (time = 0 s) with non-familiar or familiar conspecific (line [mean Z-score]; shade [SEM]). (**E, F)** Line graphs depicting 1 s average signal ± SEM. Two-way RM ANOVA, multiple comparisons test with FDR correction (ns denotes non-significance, ** denotes Q < 0.01; n=35 trials, 7 mice).

In the next set of experiments we sought to understand PVN astrocyte activity while mice (n= 35 trials; 7 mice) freely interacted with a conspecific in a homecage setting. Test mice were subjected to 3 trials of social behaviour tests: trial 1 was used as a habituation period and not used for analysis; trials 2 and 3 were interleaved with either a familiar or non-familiar same-sex juvenile mouse. Mice expressing GCaMP6f in astrocytes in a single-channel fiber photometry setup showed no significant change while sniffing a familiar or non-familiar mouse (Figure 8). Interestingly, prior to interacting with a non-familiar mouse (2 to 1 seconds before sniff) there was a significant increase in GCaMP fluorescence (Mean z-score 0.1514; Q = 0.0043). These findings provide evidence that PVN astrocytes become active prior to social sniffing interactions with a non-familiar, but not familiar, conspecific.

3.4 PVN Astrocyte and oxytocin activity changes during social sniffing

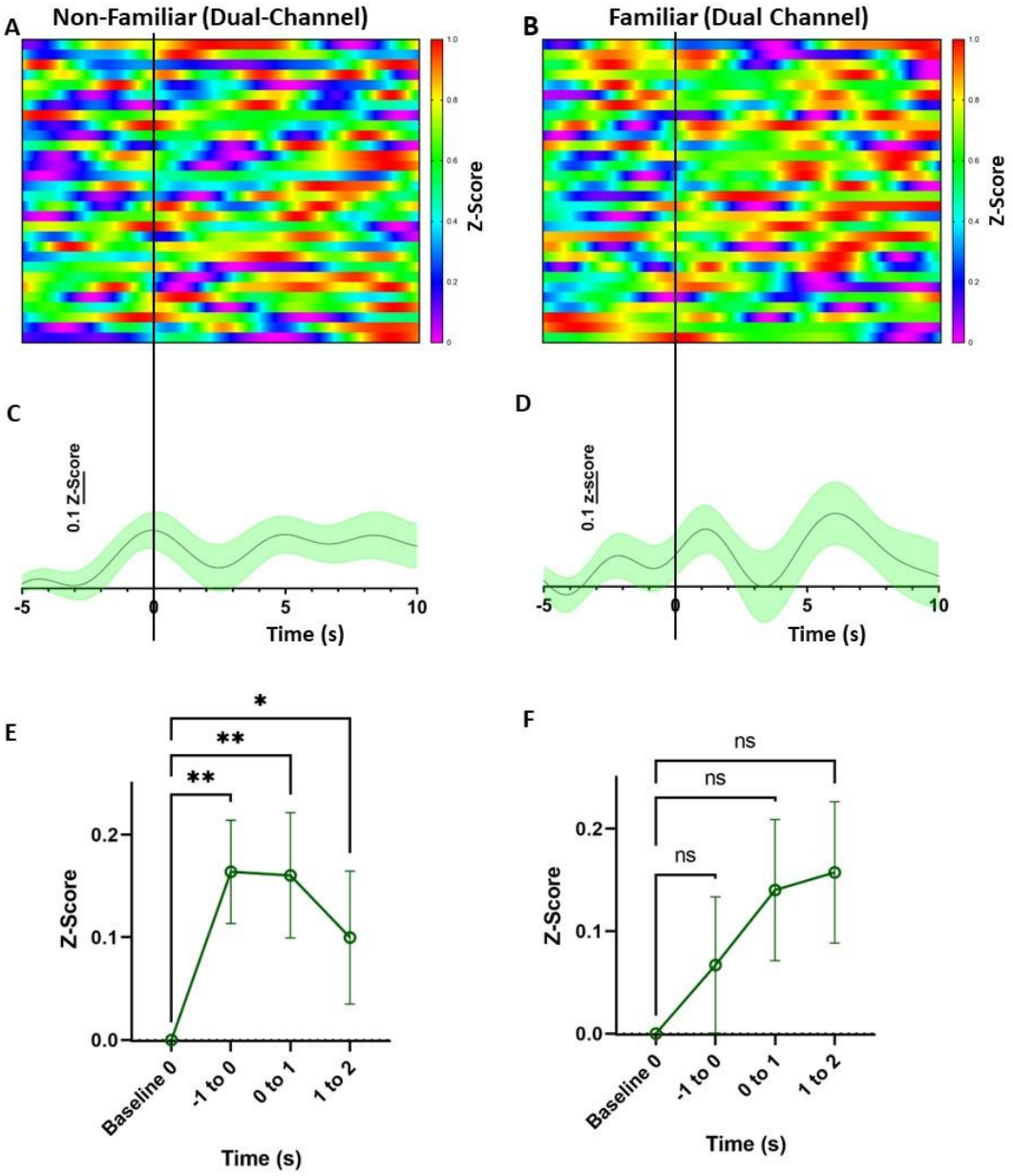

Figure 9. Calcium activity from PVN astrocytes during social sniffing in dual-channel recordings. A,B Heatmaps showing average changes in fluorescence of GCaMP6 in single-channel fiber photometry upon sniffing onset (black vertical line) of familiar or non-familiar conspecific **(C, D)** Mean (green) traces of GCaMP6 signal on onset of sniff (time = 0 s) with non-familiar or familiar conspecific (line [mean Z-score]; shade [SEM]). (**E, F)** Line graphs depicting 1 s average signal ± SEM. Two-way RM ANOVA, multiple comparisons test with FDR correction (ns denotes non-significance; * denotes Q<0.05, ** denotes Q < 0.01; n=30 trials, 6 mice).

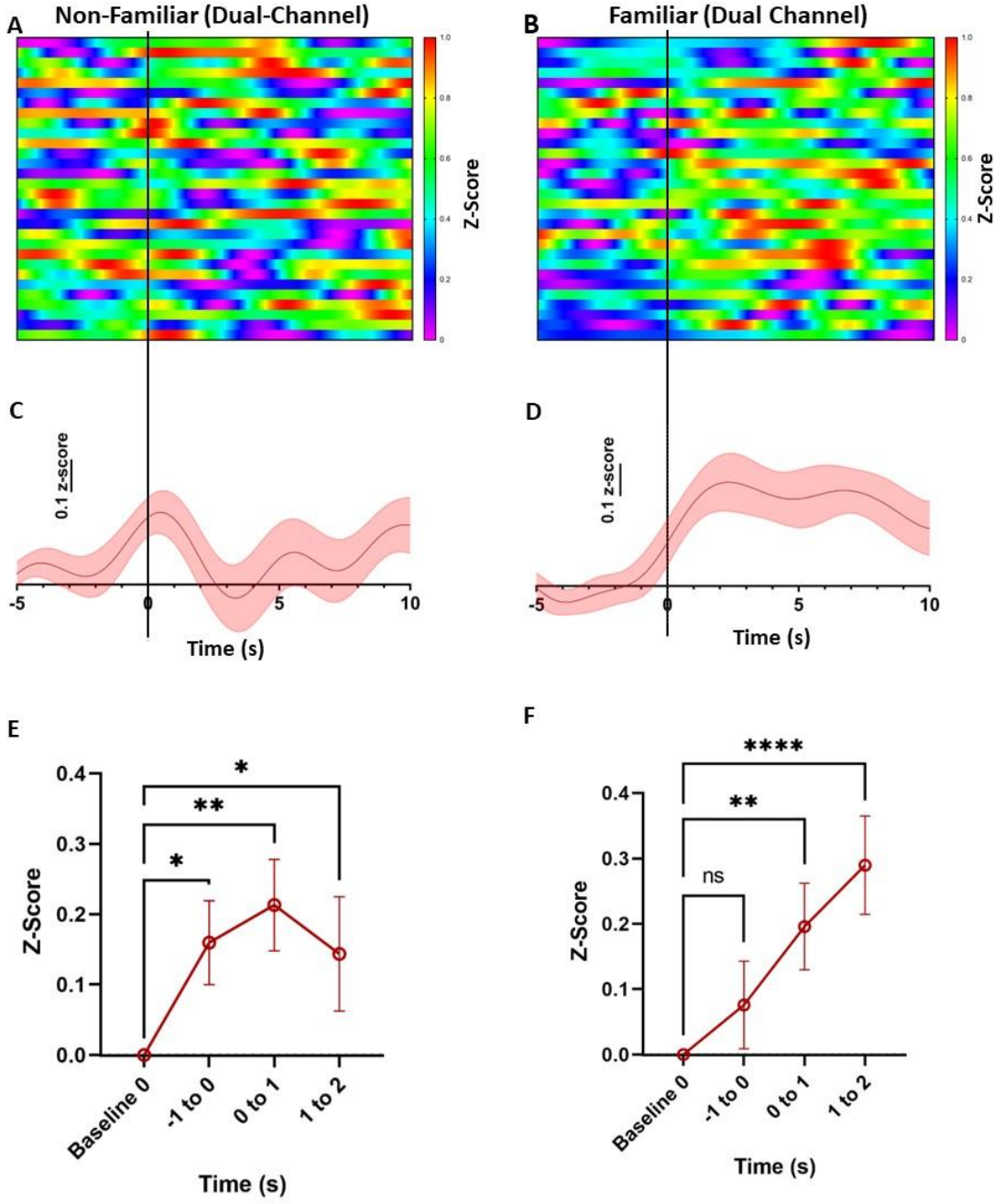

Figure 10. Calcium activity from PVN oxytocin neurons during social sniffing in dual-channel recordings. A,B Heatmaps showing average changes in fluorescence of GCaMP6 in dual-channel fiber photometry upon sniffing onset (black vertical line) of a non-familiar or familiar conspecific **(C, D)** Mean (red) traces of GCaMP6 signal on onset of sniff (time = 0 s) with a non-familiar or familiar conspecific (line [mean Z-score]; shade [SEM]). (**E, F)** Line graphs depicting 1 s average signal ± SEM. Two-way RM ANOVA, multiple comparisons test with FDR correction (ns denotes non-significance; * denotes Q<0.05, ** denotes Q < 0.01, **** denotes Q<0.0001; n=30 trials, 6 mice).

To simultaneously monitor the activity of PVN OXT neurons and astrocytes during social interactions, we performed the same social experiment as above (Section 3.3) in Oxt-Cre mice (n= 30 trials; 6 mice). Oxt-Cre mice expressed Cre-dependant RCaMP2 in PVN OXT neurons and GCaMP6 in PVN astrocytes. Similar to our previous findings, we found that GCaMP6 fluorescent signals significantly increased prior to social sniffing interactions with a non-familiar, but not familiar, conspecific (figure 10; mean z-score at -1 to 0 seconds = 0.1637; Q=0.0030). Interestingly, in these mice we found that the increase in GCaMP6 signal persisted during, and after, the social interaction which contrasts with our single-channel recordings in Section 3.3 (mean z-score at 0 to 1s = 0.1602; Q=0.0071). This provides further evidence that PVN astrocytes increase in activity prior to a social sniffing interaction with a non-familiar but not familiar conspecific. The interesting finding that in dual-channel mice the activation of PVN astrocytes persisted for a longer period is potentially possible due to the social interaction dynamics that occurred between mice in this set of specific experiments (for further explanation, see Discussion Section 4.1). In RCaMP2 recordings, we found that both familiar and non-familiar conspecifics induced an increase in fluorescent signal (Figure 10). With non-familiar mice the increase in RCaMP2 signal began 1 second prior to social sniffing (mean z-score = 0.1594; Q = 0.0246), peaked during the sniff (0 to 1 second; mean z-score 0.2130; Q = 0.0042), and persisted until the 1-2 second time point (mean z-score = 0.1434; Q = 0.0308). Interestingly, social sniffing with a familiar conspecific did not produce a significant increase in RCaMP2 fluorescence prior to the sniff (mean peak = 0.07559; Q = 0.0870) but showed a strong significance during the sniff (mean peak = 0.1957; Q = 0.0016) which continued to increase after the sniff

(mean peak at 1-2 seconds = 0.2896; $Q < 0.0001$). These findings provide us with the expectant result that PVN OXT neurons increase in activity during social sniffing. Although, there are two unexpected findings in our dual-channel recordings. Firstly, OXT neuron activity increased prior to sniffing with a non-familiar, but not familiar mouse (Figure 10). As PVN astrocytes also increase at this time point with non-familiar mice, it is possible that these two cell types interact during non-familiar, but not familiar interactions. Secondly, the increase seen in PVN OXT neurons persists long after a social sniffing interaction has begun with a familiar mouse (Figure 10). Although, this finding is possibly due to multiple social interactions in a short period of time after the initial social sniff, as familiar mice tended to interact in multiple bursts of social interactions (data not shown).

3.5 PVN astrocytes increase in activity following looming shadow task

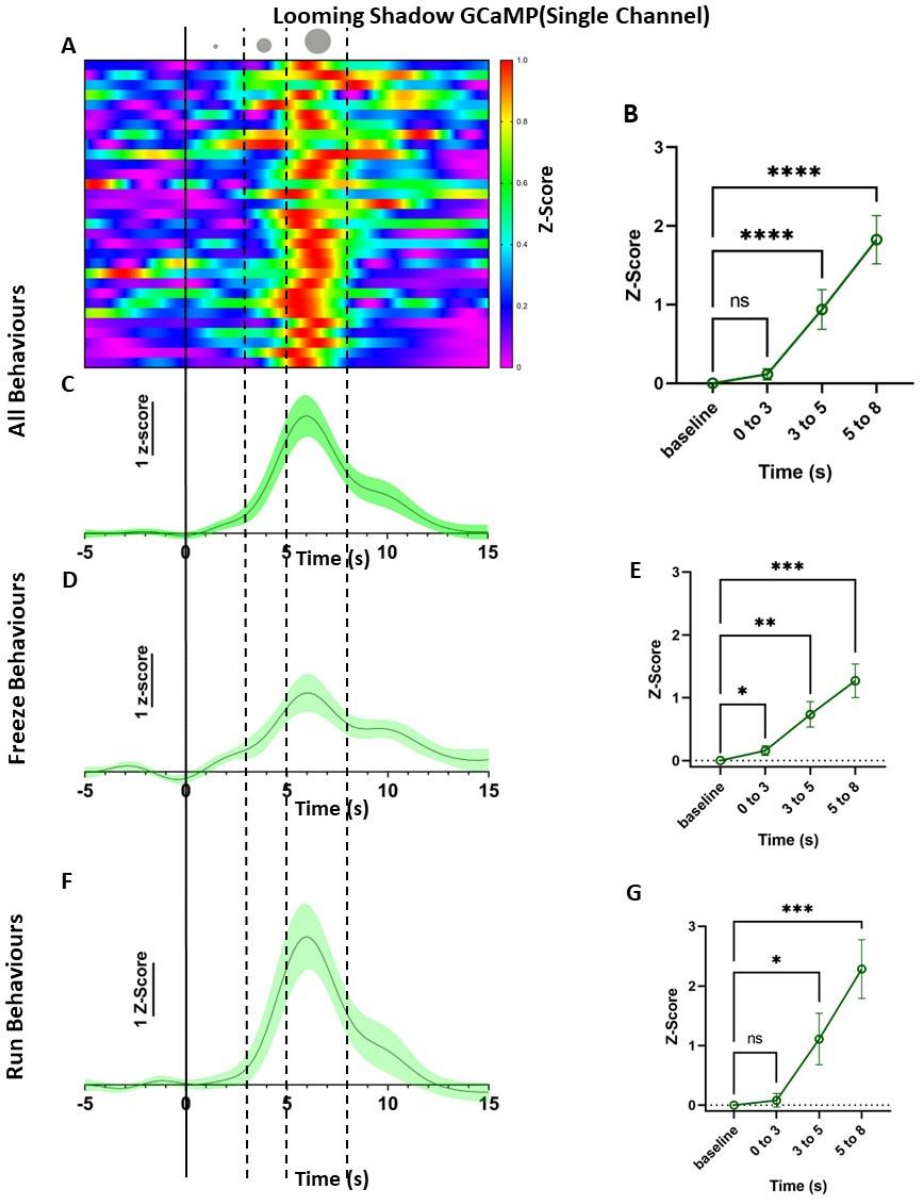

Figure 11. Calcium activity from PVN astrocytes during looming shadow task in single-channel recordings. A Heatmap depicting changes in GCaMP fluorescence during the 3 phases of the looming shadow task (3 phases depicted above heatmap; (steady 0-3s, growth 3 to 5s, looming 5-8s) **B, E, G** Mean z-scores when compared to baseline during 3 phases of looming shadow task **C, D, F** Traces depicting change in GCaMP fluorescence upon looming shadow appearance (t=0 s) for all behaviours (**C; n=31 trials**) or divided into individual Freeze (**D; n=14 trials**) and Run (**F; n=17 trials**) behaviours. (Two-way RM ANOVA with FDR correction). (ns denotes non-significance; * denotes Q < 0.05, ** denotes Q < 0.01, *** denotes Q = 0.0001, **** denotes Q < 0.0001; n= 8 mice).

To evaluate PVN astrocyte responses to stress stimuli, 8 mice (31 trials) were subjected to the looming shadow stress task. This task was designed to allow the mouse subject to make a decision while under stress from a perceived threat from above while allowing for fiber photometry recordings via a head-attached fiber optic cable. When triggered, a small dot first appears on a monitor above the mouse (0 to 3s). The shadow then expands for 2 seconds before looming for 3 seconds before disappearing (total time 8 seconds). During these sessions, mice displayed 1 of 3 behaviours: Freeze in place, run under a small house for safety, or not respond to the artificial threat. The few instances where a mouse did not perform a freeze or run behaviour were excluded from data analyses as these did not elicit a stress response and the mouse was potentially unaware of the stimulus. Mice expressing GCaMP6 in PVN astrocytes showed an increase in fluorescent signal 3-8 seconds after the appearance of the looming shadow while peaking during the looming phase (looming phase: 5-8s; Figure 11. A, B, C; mean z-score = 1.825; $Q < 0.0001$). Freeze and run behaviours were then divided to determine if there are any alterations in GCaMP fluorescent signal depending on the behaviour being performed. Freeze behaviours showed a significant increase during all 3 of the looming shadow phases (Figure 11. D, E). Interestingly, during freeze behaviours we saw a significant increase in GCaMP6 signal during the steady phase (0-3s; mean z-score 0.1576; $Q = 0.0247$) which we did not see when combining all behaviors. We also did see a significant increase during the growth phase (3-5s; mean peak 0.7341; $Q = 0.0008$) and looming phase (5-8s; mean peak 1.269; $Q = 0.0004$). In contrast to this we did not see an increase in GCaMP6 signal during the steady phase (mean peak = 0.08071; $Q = 0.0859$) when mice ran from

the shadow (Figure 11. F, G). However, we did see the expected increase in GCaMP6 signal during the growth (mean z-score = 1.109; Q = 0.0043) and looming phase (mean z-score = 2.283; Q = 0.0001) during run behaviours. It is interesting to note that the increases seen in GCaMP6 signal during run behaviours is of greater value than during freeze, or all behaviours combined. This is potentially due to the fact that during freeze behaviours, the increases seen in GCaMP6 signal are less coordinated than when mice ran from the shadow. This can be seen in the heatmap provided (Figure 11. A), as the top 14 trials are of mice freezing from the shadow and these trials appear “out of sync” when compared to the general population of trials, or during run behaviours.

3.6 PVN astrocytes but not oxytocin neurons respond to the looming shadow task

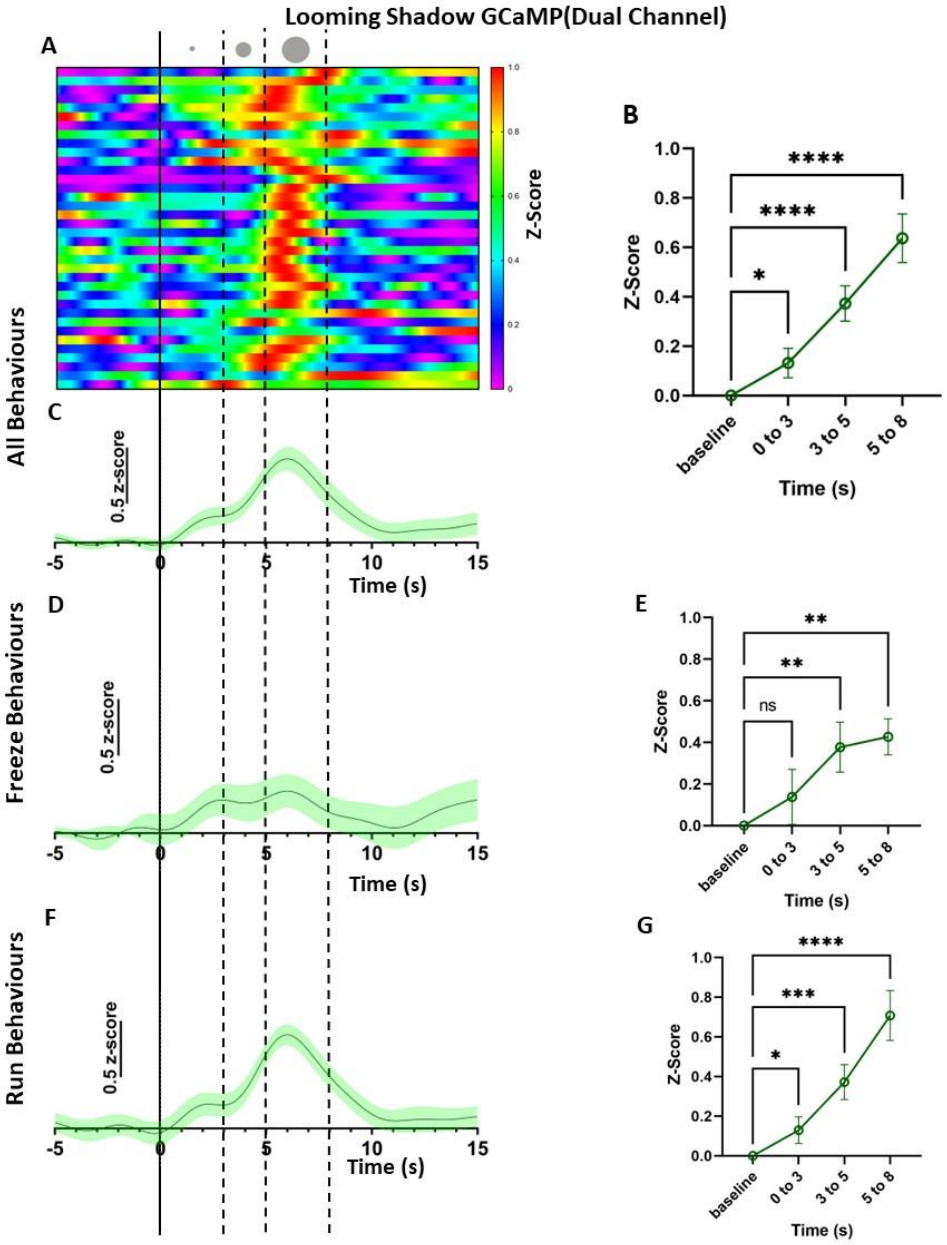

Figure 12. Calcium activity from PVN astrocytes during looming shadow task in dual-channel recordings. A Heatmap depicting changes in GCaMP6 fluorescence upon appearance and growth of looming shadow. **B, E, G** Mean z-scores when compared to baseline during 3 phases of looming shadow task (steady 0-3s, growth 3 to 5s, looming 5-8s) **C, D, F** Traces depicting change in GCaMP6 fluorescence upon looming shadow appearance (t=0) for all behaviours (**C n=37 trials**) or divided into individual Freeze (**D n=10 trials**) and Run (**F n=27 trials**) behaviours. (Two-way RM ANOVA with FDR correction). (ns denotes non-significance; * denotes Q < 0.05, ** denotes Q < 0.01, *** denotes Q = 0.0001, **** denotes Q < 0.0001; n=9 mice).

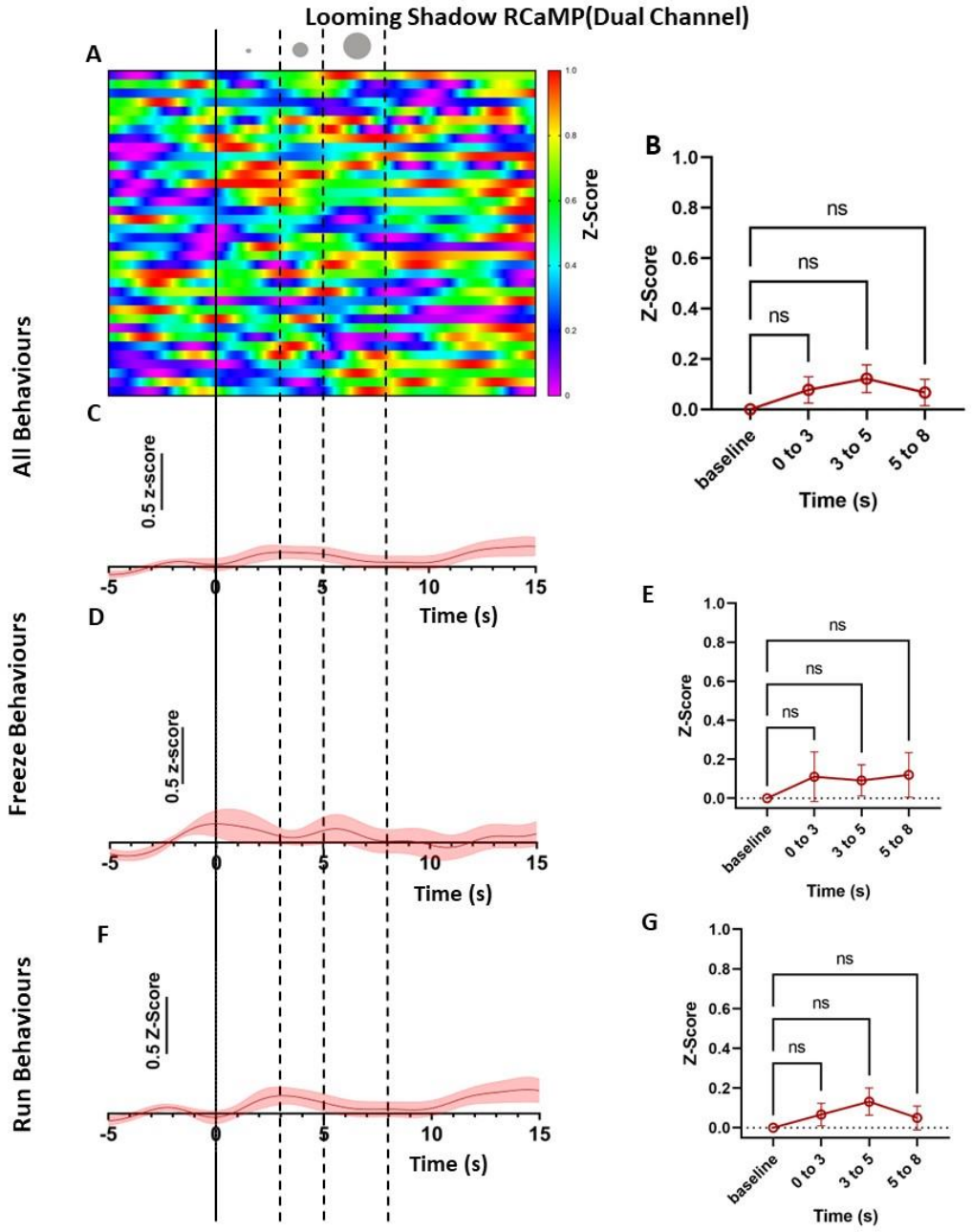

Figure 13. Calcium activity from PVN oxytocin neurons during looming shadow task in dual-channel recordings. A Heatmap depicting changes in GCaMP6 fluorescence upon appearance and growth of looming shadow. **B, E, G** Mean z-scores when compared to baseline during 3 phases of looming shadow task (steady 0-3s, growth 3 to 5s, looming 5-8s) **C, D, F** Traces depicting change in RCaMP2 fluorescence upon looming shadow appearance (t=0) for all behaviours (**C, n=37**) or divided into individual Freeze (**D, n=10**) and Run (**F, n=27**) behaviours. (Two-way RM ANOVA with FDR correction). (ns denotes non-significance; 9 mice).

Simultaneous fiber photometry recordings of PVN astrocyte and OXT neuron calcium activity were then performed using the Oxt-Cre mice expressing GCaMP6 in astrocytes and RCaMP2 in OXT neurons. As expected based on previous results, we found that GCaMP6 fluorescence significantly increased during the looming shadow task during the growth (3-5s; mean z-score 0.3726, $Q < 0.0001$) and looming phases (5-8s; mean z-score 0.6374, $Q < 0.0001$; Figure 12. A, B, C). In contrast to our previous findings (Section 3.5), we saw a significant increase in GCaMP6 signal during the steady phase (0-3s; mean z-score 0.1318, $Q = 0.0087$). We then parsed out GCaMP6 signals based on whether the mouse froze or ran during their trials. When we examined GCaMP6 fluorescent signals when mice froze from the looming shadow, we saw a significant increase during the growth (mean z-score 0.3768, $Q = 0.0072$) and looming (mean z-score 0.4269, $Q = 0.0012$) phases of the looming shadow task (Figure 12 D, E). During run behaviours, GCaMP6 fluorescent signals increased during the steady (mean peak = 0.1299, $Q = 0.0225$), growth (mean peak = 0.3720, $Q = 0.0001$), and looming (mean peak = 0.7076, $Q < 0.0001$) phases of the looming shadow task (Figure 12. F, G). As we found an unexpected significant increase in GCaMP6 fluorescent signal during the steady phase when mice ran from the shadow, we suspect this drove the significant increase in signal when we combined all trials together. These findings provide further evidence that PVN astrocytes are active during the looming shadow task, as we saw previously in section 3.5.

In PVN OXT neuron recordings we found that there was no significant increase in RCaMP2 fluorescent signal in any of the 3 phases of the looming shadow task (Figure 13. A, B, C). Although we did find that RCaMP2 fluorescent signal non-

significantly trends in the positive direction during the growth phase (3-5s; mean z-score = 0.1219, Q = 0.4348). We further categorized RCaMP2 signal based on the behaviour performed by the mouse to determine if a specific behaviour is behind this positive trend, and whether this trend is significant when removed from the other behaviour. First, we looked at freeze behaviours. We found that similarly to 'all behaviours', freeze behaviours showed no significant increase during any phases of the looming shadow task and that the positive upwards trend during the growth phase is gone (Figure 13. D, E). Next we looked at run behaviours. Again, we found that there is no significant increase during any of the three phases of the looming shadow task (Figure 13. F, G). Interestingly, we did see the positive trend during the growth phase (mean z-score 0.1320, Q = 0.1791). These findings show us that PVN OXT neurons are not active during the looming shadow task, but the interesting positive trend we see during the growth phase (when mice run from the looming shadow) may provoke future studies to investigate sub-groups of PVN OXT neurons to determine if a sub-group of PVN OXT neuron is active during run responses to the looming shadow task.

3.7 PVN astrocytes but not OXT neurons are active during tail lift

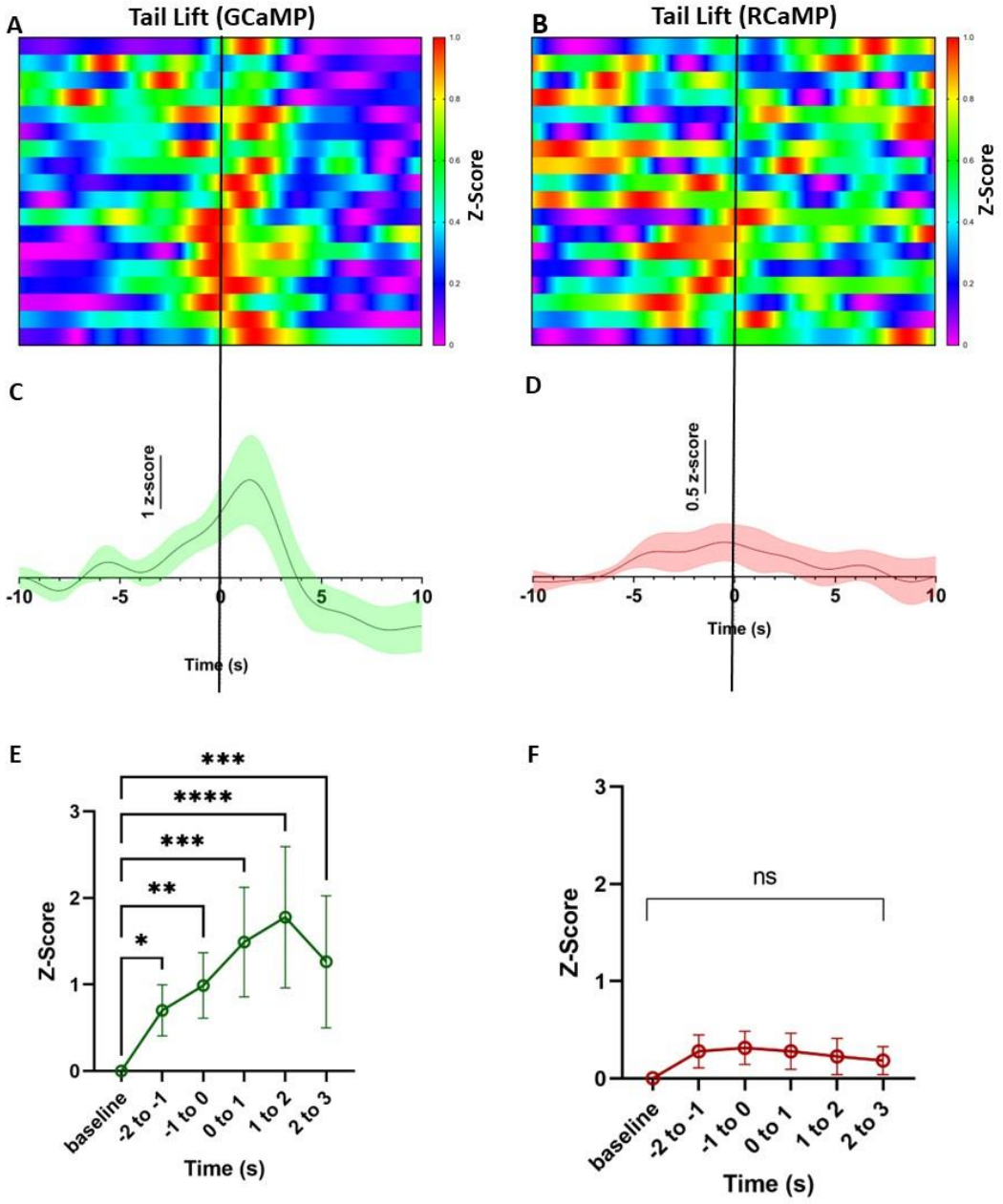

Figure 14. Calcium activity from PVN astrocytes and oxytocin neurons during tail lift. A,B Heatmaps depicting changes in GCaMP6 (**A**) and RCaMP2 **(B)** fluorescence during tail lift procedure. **C, D** Traces depicting change in GCaMP6 (Green, **C**) and RCaMP2 (Red, **D**) fluorescence upon tail lift (t=0). **E, F** Average z-scores compared to baseline during tail lift procedure. Two-way RM ANOVA with FDR correction. (ns denotes non-significance; * denotes Q < 0.05, ** denotes Q < 0.01, *** denotes Q = 0.0001, **** denotes Q < 0.0001; n=18 trials, 9 mice).

The tail lift is an easy way to induce stress upon a mouse that does not offer the mouse a choice in how to respond. The tail lift also allowed us to view the stress response within PVN astrocytes and OXT neurons in an uncontrollable situation (Daviu et al., 2020). 9 Oxt-Cre mice expressing GCaMP6 in astrocytes and RCaMP2 in OXT neurons were subjected to tail lift over 2 trials on separate days during dual-channel recordings of PVN astrocytes and OXT neurons (Figure 14). During the tail lift procedure we found that there was a significant increase in GCaMP6 signal at least 2 seconds prior to (-2 to -1s mean z-score = 0.7013, Q = 0.0169), during (0 to 1s mean z-score 1.492, Q = 0.0001), and after the tail lift (Figure 14. A, C, E). The mean peak response in GCaMP6 signal was seen at the 1 to 2 second period after the onset of touching the mouse tail to lift (mean z-score 1.778, Q < 0.0001) and persisted until the 2 to 3s time period (mean z-score 1.263, Q = 0.0006). It is of note that some mice showed an early response in GCaMP6 signal, at least 3 seconds prior to the tail lift; this is potentially due to handler difficulties when attempting to grasp the mouse tail (can be seen in heatmap Figure 14. A). It is also important to note that early-responding mice did indeed still show an increase (although smaller) during the actual tail lift procedure (Figure 14. A). PVN OXT neurons on the other hand showed no significant change in RCaMP2 fluorescent signal during the tail lift procedure (Figure 14. B, D, F). Interestingly, there was a small positive deflection in RCaMP2 signal which peaked prior to the tail lift (-1 to 0 mean z-score 0.3115, Q = 0.6830). It is important to note that mice often ran from the experimenter's oncoming hand before being picked up by the tail (data not shown). Therefore, the positive deflection seen during the tail lift procedure does share similarities with the non-significant positive trend seen during looming

shadow run behaviours (Section 3.6) and may warrant further investigation to identify potential PVN OXT neuron subgroups involved in stress-related run behaviours. The results found during the tail lift procedure provide further evidence to the results we have seen in previous sections 3.5 and 3.6, in that PVN astrocytes are active during the stress response while PVN OXT neurons are not.

4. Discussion

4.1 PVN Astrocytes during Social and Stress Tasks

In this current study we used single- and dual-channel fiber photometry to better understand the dynamics between PVN astrocytes and OXT neurons during social and stress contexts. We employed the social odour preference test, the reciprocal social interaction task, the looming shadow task, and a tail lift procedure. We initially found that PVN astrocytes are not active while a mouse sniffs a social, or a non-social (almond) odour in single-channel fiber photometry recordings (Section 3.1). We followed up this result with dual-channel recordings of PVN astrocytes to confirm that PVN astrocytes are not active during social and non-social odour sniffing (Section 3.2). We then performed reciprocal social interaction tests and found that PVN astrocytes increase in activity before and during sniffing of a non-familiar, but not a familiar, juvenile mouse (Sections 3.3 and 3.4). Previous research has found that CRH neuron mediated AVP release activates PVN astrocytes during stress to provide a local positive and/or negative feedback mechanism to modulate continued CRH neuron activation (Chen et al., 2019). Therefore, it is probable that the activation seen in PVN astrocytes prior to sniffing a non-familiar conspecific correlates with the stress induced when interacting with a novel mouse for the first time. This mild social stress causes an increase in CRH neuron mediated AVP release on to PVN astrocytes which likely produces the increase in activity we see in our recordings (Figure 8). It is important to note that we do see a temporal difference in the activation of PVN astrocytes between single- and dual-channel recordings. During single-channel recordings, we see a

significant increase in PVN astrocyte activity during the -2 to -1 second time periods, before the sniff occurs (Section 3.3). In contrast to this we see a significant increase in PVN astrocyte activity during the -1 to 2 seconds prior to, and after the sniff occurs (Section 3.4); this is a longer and later time frame than single-channel recordings. There are at least three possible reasons why this could occur. Firstly, it is possible that the later, and longer response seen is caused by a bleed-through effect between the two recording LEDs during dual-channel recordings. Although this is unlikely for 2 reasons: First, GCaMP6 absorbs wavelengths of about 450 – 510 nm and emits wavelengths of about 500 – 550 nm, while RCaMP2 absorbs wavelengths of about 520 – 600 nm and emits light of about 570 – 670 nm (Lambert, 2022). Therefore, it is unlikely that the RCaMP2 emittance in the 570 – 670 nm range is causing the increase in GCaMP6 signal being recorded in the 500 – 550 nm range. Secondly, we would expect all large increases in RCaMP2 signal to reflect in GCaMP6 signal and we do not see this effect in familiar social sniff tests, as RCaMP2 signals show a strong response while GCaMP6 signals show no response. The second possible reason for the time delay that we see between single- and dual- channel recordings during social sniffing is the social dynamics between the two mice during the social sniff. It is possible that our single-channel mice happened to have more positive social interactions with their non-familiar conspecific while the dual-channel mice had more negative social interactions such as aggression and fighting behaviour. This would explain the longer PVN astrocyte activity seen in dual-channel mice, as AVP mobilization is implicated in murine aggressive behaviours (Veenema et al., 2006). A negative social interaction could lead to increased AVP release onto PVN astrocytes, and this increase would lead to the prolonged PVN

astrocyte activity we see in Section 3.4. One way to reduce this factor would be to increase the number of mice being tested, this would reduce any effect a positive, or negative social interaction has on the overall recordings. Another way would be to categorize and analyze positive and negative interactions separately. Not only would this be able to help explain the differences we see here, but this would also provide more insight into PVN astrocyte activity during complex social interactions. The difficulty here may be defining a positive interaction vs. a negative interaction and determining when each occurs. The third, and most likely reason could be sex differences. During single-channel recordings we recorded from 7 male mice whereas in dual-channel recordings we recorded from 3 males and 3 females (Methods Section 2.1). It is possible that the PVN astrocyte response occurs quicker and for a shorter time period in the male mouse, compared to the female response. Based on previous literature, this potential sexual dimorphism may be CRH neuron mediated. A study by Senst et al., (2016) employed whole-cell patch clamp to look at social isolation and acute stress effects on the male and female mouse PVN CRH neuron activity. Senst et al., found that although a 20-minute forced swim test did not cause sexually dimorphic effects on CRH neuron electrical properties, social isolation did. Furthermore, there are known to be large differences in PVN AVP and OXT circuitry and activity between males and females (Scott et al., 2015; Simerly, 1998; Smith et al., 2019; Karisetty et al., 2017; Rigney et al., 2021). It is possible that there are large differences in PVN circuitry between CRH, OXT, AVP neurons and astrocytes for social activities. Therefore, we would expect to see a longer response in dual-channel recordings of the two sexes, as the male mouse PVN astrocytes may respond before the social sniff occurs, while the

female mouse PVN astrocyte response may occur during and/or after sniff occurrence. These two separate increases in activity levels would cause an elongated signal, like what we see in our dual-channel social recordings (Section 3.4). Our next step would be to perform a sub-analysis of dual-channel recorded male mice to examine whether we observe similar results to single-channel recorded male mice. It would also be important to increase the number of female mice being recorded in single-channel PVN astrocyte recordings to elucidate this potential sexual dimorphism in PVN astrocyte response during social sniffing.

We performed two stress tests to identify PVN astrocyte activity alterations while mice are under stress. We found that PVN astrocytes are active during the looming shadow and tail lift stress tests (Sections 3.5, 3.6, and 3.7). During single-channel recordings there was a significant increase in PVN astrocyte activity during the 3-8 second time periods with the largest increase in activity between 5-8s in the looming phase (Section 3.5). Based on previous literature, it is predicted that looming shadow stress would activate CRH neurons, then PVN astrocytes will become active, in a successive manner (Chen et al., 2019). Daviu et al. (2020) found that the largest responses in GCaMP6s signal was on average 5 seconds post-looming shadow initiation, which slightly precedes the astrocyte signal peak (5-8 seconds post shadow appearance) that we observed. It is important to note that Daviu et al., used GCaMP6s, whereas we used GCaMP6f, two fluorophores with different temporal dynamics. The temporal dynamics of GCaMP6s has been measured to be approximately 50-75 ms slower than GCaMP6f (Chen et al., 2013), the fluorophore we used in our study. Based on this information and comparing the temporal dynamics between our study and Daviu

et al., it is reasonable to assume that during the looming shadow task, PVN CRH neurons elicit a response before PVN astrocytes. Our finding confirms previous *in vitro* observations that PVN CRH neurons activate PVN astrocytes during a stress response (Chen et al., 2019), and serve as the first *in vivo* demonstration of stress-induced activity increase PVN astrocytes.

Interestingly, we found that in single-channel recording trials when mice exhibited freezing behaviours, there was an earlier increase in PVN astrocyte activity when compared to run behaviours (Section 3.5). This discrepancy could be explained by "early responders", as some mice tended to respond to the shadow earlier than others. Heatmaps in Section 3.5 show these early responders, as the top 14 trials are recordings from freeze responses and show a large variability in PVN astrocyte responses, whereas run behaviours (bottom 17 trials) do not show such variability. Based on previous research, we expected to see a significant early response in PVN astrocyte activity during run behaviours (Sections 3.5 and 3.6). Daviu et al. (2020), found that mice who had control over their defensive strategies and ran from the shadow had a distinct increase in PVN CRH neuronal activity ~2 seconds before the largest CRH neuron activity increase. In contrast to this, mice with no control over their defensive strategies, or froze in response to the shadow, did not have this pre-activity increase in PVN CRH activity. Therefore, if CRH neurons increase in activity ~2 seconds before the main activity is seen during run behaviours in the looming shadow task, we would expect AVP to be released and activate PVN astrocytes on a similar ~2 second time frame before the main PVN astrocyte activity increase. Unexpectedly, we did not see this occur during our single-channel recordings (Section 3.5), but we do see

this occur in our dual-channel recordings (Section 3.6). Our observation that run behaviours show an earlier increase in PVN astrocyte activity when compared to freeze behaviours is in good agreement with previous literature. Why we did not see a similar increase during single-channel recordings could be due to sexual dimorphism, or more likely due to differences in the length of habituation. The Daviu et al. study did not distinguish between male and female mice or note any differences between sexes when running their experiments. Therefore, it is likely that the length of habituation may play a large role in the differences we see here. Single-channel mice were initially habituated for 3 days for 10-minutes at a time, while dual-channel mice were habituated for 5 days for 10-minutes. This increased habituation period may have allowed the mice to feel more comfortable with the testing apparatus and more control over their defensive behaviours when exposed to the looming shadow. Finally, we examined PVN astrocyte activity during the tail lift stress procedure in dual-channel mice (Section 3.7). The tail lift provides further evidence that PVN astrocytes are active during uncontrollable stress response, and that this peaks at about 1-2 second after the initiation of the tail lift. In conclusion, we have found that PVN astrocytes increase in activity during the looming shadow stress test and our results are in agreement with previous literature on CRH-mediated responses in PVN astrocyte activity during the looming shadow stress task (Chen et al., 2019; Daviu et al., 2020).

4.1 PVN Oxytocin Neuron Responses during Social and Stress Tasks

In Oxt-Cre mice we employed dual-channel fiber photometry using a Cre-promotor to visualize OXT neuron activity in freely behaving mice. We first explored

whether an odour from a non-familiar mouse cage would be strong enough to elicit an increase in PVN OXT activity, but we failed to observe such an effect (Section 3.2). In contrast, we found that sniffing of a non-familiar mouse causes a significant increase in PVN OXT neuron activity (Section 3.4). We therefore believe that odour alone is not a strong enough stimulus to cause a fiber photometry-detectable activity increase PVN OXT neurons. It would be interesting to further our study by providing visual and olfactory stimulation related to a mouse to test if this will elicit the same response we see in our social sniffing experiments. If these stimuli elicit a detectable OXT response, this would suggest that PVN OXT neurons require the convergence of multiple social stimuli to increase PVN OXT activity.

We also found that while mice sniffed the non-social (almond) scent, there was a significant decrease in PVN OXT neuron activity (Section 3.2). This unexpected result is potentially due to the appetitive almond scent used in the study. Previous findings have found mixed results related to whether OXT neurons are involved in feeding behaviours (Atasoy et al., 2012; Wu et al., 2012; Sutton et al., 2014). Recently, Chen et al. (2022) suggested a potential avenue to reconcile these variable results. Chen et al. combined electrophysiological recordings, morphological reconstructions, and unsupervised clustering analyses on 224 PVN OXT neurons from 23 mice to identify 6 distinct populations of PVN OXT neurons (Chen et al., 2022). They were then able to identify that subgroup “ME-2b” (interestingly, is comprised of both parvOXT and magnOXT neurons located in the posterior PVN) is involved in feeding cessation. This finding is furthered by a study by Iwasaki et al. (2019) who found that i.p. injections of an OXTr antagonist increased feeding in mice, whereas an OXTr agonist induced the opposite

effect. Therefore, it is possible that the almond scent that we used in our experiments as a non-social odour induced appetitive behaviour in mice, and this caused the decrease in PVN OXT neurons activity we see here. Therefore, these unexpected findings provide further evidence that PVN OXT neurons reduce in activity during appetitive behaviours.

We found that during reciprocal social interaction tests, PVN OXT neuron activity significantly increased during social sniffing with a familiar and a non-familiar mouse (Section 3.4). This is an expected result as previous research has found that OXT is important for pro-social behaviours and acts as a "social switch" for the brain when interacting with a conspecific (Lewis et al., 2020; Jurek and Neumann, 2018). Our findings are in agreement with previous literature, as a recent study by Tang et al. (2020) recorded individual PVN OXT neurons *in vivo* during freely behaving social interactions. Tang et al. had found that PVN OXT neurons increase in firing activity during social interactions when compared to an empty open-field box. Interestingly, we do see that social sniffing with a familiar mouse induced a longer increase in PVN OXT neuron activity than with a non-familiar mouse. It is possible that familiarity and non-familiarity cause different groups of PVN OXT neurons to be active, and a larger population of PVN OXT neurons are active during a familiar social interaction. An experiment performed by Arakawa et al. had found that OXT infusion into male mice reduced territorial marking with non-familiar mice and the odour of pair-housed mice produced a similar effect. The authors conclude that OXT is important in regulating social familiarity based on odour cues (Arakawa et al., 2015). Based on these findings we would expect to see a greater mobilization of OXT during familiar interactions and

this greater mobilization of OXT coincides with an increase in PVN OXT neuron activity, as OXT neurons are known to possess autocrine capabilities (Jurek & Neumann, 2018). In non-familiar tests, we see an earlier and shorter activation of PVN OXT neurons. This can be explained as a small group of PVN OXT neurons become active then deactivate as soon as socialization ends. On the other hand, a familiar conspecific increases the activity of a group of PVN OXT neurons, which then activate other groups of PVN OXT neurons, creating the longer period of activation seen in our data (Section 3.4). This could be further studied by repeating fiber photometry recordings of PVN OXT neurons in reciprocal social interaction tests, as we performed in our experiments, but over 5 sessions with the same (initially non-familiar) mouse. This would allow for familiarity to increase between mice over the 5 sessions. Then experimenters could then compare PVN OXT activity during social sniffing across each of the 5 sessions and expect to see longer activity increases in the last session, when compared to the first session. This would provide evidence of PVN OXT neuron recruitment as familiarity increases. Another possible way to investigate this hypothesis is by employing the use of a mini-scope. The mini-scope would allow for the visualization of individual neurons with a high spatial resolution and could uncover groups of neurons that are active during familiar, and non-familiar social interactions.

Finally, we analyzed PVN OXT neuron activity as mice underwent the looming shadow and tail lift stress tasks (Sections 3.6 and 3.7). We were surprised to find that there was not a significant increase in PVN OXT neuron activity during any of the stress tests employed. This contrasts with previous studies who have found that PVN OXT neurons are active, and OXT is released within the PVN during various stressors

(Section 1.4.4; Lang et al., 1983; Nishioka et al., 1998; de Jong et al., 2015; Engelmann et al., 2001; Windle et al., 1997; Wotjak et al., 2001). It is of note that we do see a non-significant positive trend in PVN OXT neuron activity during the looming shadow task at the 3-5s time period (during shadow growth) when mice ran from the shadow and a similar trend during the tail lift procedure (Sections 3.6 and 3.7). As the literature strongly suggests that PVN OXT neurons are active during stress, it is likely that there is a sub-population of PVN OXT neurons that are activate during our stress tasks. This sub-population may be difficult to detect within the whole population of PVN OXT neurons using our methods, since our fiber photometry recordings target the whole population of PVN OXT neurons. Therefore, it is necessary to employ a technique with a higher resolution to better identify PVN OXT sub-population activity during stress tasks, such as mini-scope recordings during behaviour experiments.

4.3 PVN Astrocyte and Oxytocin Neuron Dynamics in Social and Stress

We performed dual-channel fiber photometry recordings to visualize PVN astrocytes and OXT neurons *in vivo* during freely-behaving tasks with an aim to uncover the dynamics between these two cell types. During social sniffing with a non-familiar conspecific, we see a significant increase in both PVN astrocyte and OXT neuron activity (Section 3.4). Interestingly, the largest mean activity increase we see in PVN astrocytes appears prior to the sniff at the -1 to 0 second period while PVN OXT neuron's largest mean activity is 0 to 1 seconds, after the sniff occurred. This finding provides evidence against our hypothesis that PVN OXT neurons activate PVN astrocytes via OXT release, as we would expect PVN astrocyte activity increases after

PVN OXT activity and not before. During the looming shadow task we found that PVN OXT neurons showed a non-significant positive trend during shadow growth. Although not significant, we speculate that a small population of PVN OXT neurons are involved in run behaviours during the looming shadow task, and that this correlates with the initial increase in PVN astrocyte activity in controllable stress and run behaviours (Section 4.1). It is unlikely that we can confirm these predictions with our current technique. Our experimental design used two different fluorophores: RCaMP2 for OXT neurons, and GcaMP6f for astrocytes. To our knowledge, there is currently no literature comparing the temporal dynamics between GcaMP6f and RcaMP2 fluorophores. Nevertheless, these two fluorphores are expected to have different temporal dynamics that could alter any time-dependent differences we see between these two cell types. Therefore, a more time-dependent technique may be required to fully understand the dynamics between PVN astrocytes and OXT neurons. Optogenetics in conjunction with fiber photometry may be of better use when designing future experiments (Vesuna et al., 2020). This would allow for the activation, or inhibition of one cell type while recording from another cell type. We could then use this information to not only identify cross-talk between these two cell types but the behaviours elicited from the activation, or inhibition of PVN astrocytes and OXT neurons.

4.2 Conclusion

In conclusion, we performed single- and dual-channel fiber photometry recordings on mice during an odour preference test, freely behaving reciprocal interaction tests, a looming shadow test, and a tail lift procedure. During the odour

preferences test we had unexpectantly found that PVN OXT neurons decrease in activity as the mouse sniffs the non-social odour. This is likely caused by the appetitive almond odour used. In contrast to this, social odour sniffing did not cause any alterations in PVN OXT neuron activity. PVN astrocytes did not alter in activity while mice sniffed the social, or non-social odour. During freely-behaving social interaction tests we had expectantly found that PVN OXT neurons increase in activity during social sniffing a familiar and non-familiar mouse. Although PVN astrocytes did not alter in activity while mice sniffed a familiar mouse, PVN astrocytes did increase in activity moments before a mouse sniffed a non-familiar conspecific. During looming shadow stress tasks, PVN OXT neurons unexpectedly did not significantly increase in activity. On the other hand, PVN astrocytes did increase in activity as expected. Finally, during the tail lift procedure, PVN astrocytes increased in activity while PVN OXT neurons did not. These findings provide more evidence that PVN astrocytes are active during stress responses and PVN OXT neurons are active during socialization and decrease in activity during appetitive odours. Further experimentation will need to be completed to identify the dynamics between PVN astrocytes and OXT neurons.

References

A sexually dimorphic hypothalamic circuit controls maternal care and oxytocin secretion | Nature. (n.d.). Retrieved August 16, 2022, from https://www.nature.com/articles/nature15378

Aguilera, G., & Rabadan-Diehl, C. (2000). Vasopressinergic regulation of the hypothalamic–pituitary–adrenal axis: Implications for stress adaptation. *Regulatory Peptides*, *96*(1), 23–29. https://doi.org/10.1016/S0167-0115(00)00196-8

Aguilera, G., Subburaju, S., Young, S., & Chen, J. (2008). The Parvocellular Vasopressinergic System and Responsiveness of the Hypothalamic Pituitary Adrenal Axis during Chronic Stress. *Progress in Brain Research*, *170*, 29–39. https://doi.org/10.1016/S0079-6123(08)00403-2

Alescio-Lautier, B., Paban, V., & Soumireu-Mourat, B. (2000). Neuromodulation of memory in the hippocampus by vasopressin. *European Journal of Pharmacology*, *405*(1), 63–72. https://doi.org/10.1016/S0014-2999(00)00542-2

Althammer, F., & Grinevich, V. (2018). Diversity of oxytocin neurones: Beyond magno- and parvocellular cell types? *Journal of Neuroendocrinology*, *30*(8), e12549. https://doi.org/10.1111/jne.12549

Anpilov, S., Shemesh, Y., Eren, N., Harony-Nicolas, H., Benjamin, A., Dine, J., Oliveira, V. E. M., Forkosh, O., Karamihalev, S., Hüttl, R.-E., Feldman, N., Berger, R., Dagan, A., Chen, G., Neumann, I. D., Wagner, S., Yizhar, O., & Chen, A. (2020). Wireless Optogenetic Stimulation of Oxytocin Neurons in a Semi-natural Setup Dynamically Elevates Both Pro-social and Agonistic Behaviors. *Neuron*, *107*(4), 644-655.e7. https://doi.org/10.1016/j.neuron.2020.05.028

Arakawa, H., Blanchard, D. C., & Blanchard, R. J. (2015). Central oxytocin regulates social familiarity and scent marking behavior that involves amicable odor signals between male mice. *Physiology & Behavior*, *146*, 36–46. https://doi.org/10.1016/j.physbeh.2015.04.016

Astwood, E. B. (2013). *Recent Progress in Hormone Research: Proceedings of the 1968 Laurentian Hormone Conference*. Academic Press.

Atasoy, D., Betley, J. N., Su, H. H., & Sternson, S. M. (2012). Deconstruction of a neural circuit for hunger. *Nature*, *488*(7410), 172–177. https://doi.org/10.1038/nature11270

Bartz, J. A., Zaki, J., Bolger, N., & Ochsner, K. N. (2011). Social effects of oxytocin in humans: Context and person matter. *Trends in Cognitive Sciences*, *15*(7), 301–309. https://doi.org/10.1016/j.tics.2011.05.002

Beurel, E., & Nemeroff, C. B. (2014). Interaction of stress, corticotropin-releasing factor, arginine vasopressin and behaviour. *Current Topics in Behavioral Neurosciences*, *18*, 67–80. https://doi.org/10.1007/7854_2014_306

Bielsky, I. F., Hu, S.-B., Ren, X., Terwilliger, E. F., & Young, L. J. (2005). The V1a Vasopressin Receptor Is Necessary and Sufficient for Normal Social Recognition: A Gene Replacement Study. *Neuron*, *47*(4), 503–513. https://doi.org/10.1016/j.neuron.2005.06.031

Bielsky, I. F., Hu, S.-B., Szegda, K. L., Westphal, H., & Young, L. J. (2004). Profound Impairment in Social Recognition and Reduction in Anxiety-Like Behavior in Vasopressin V1a Receptor Knockout Mice. *Neuropsychopharmacology*, *29*(3), 483–493. https://doi.org/10.1038/sj.npp.1300360

Blevins, J. E., Schwartz, M. W., & Baskin, D. G. (2004). Evidence that paraventricular nucleus oxytocin neurons link hypothalamic leptin action to caudal brain stem nuclei controlling meal size. *American Journal of Physiology-Regulatory, Integrative and Comparative Physiology*, *287*(1), R87–R96. https://doi.org/10.1152/ajpregu.00604.2003

Brady, K. T., & Sinha, R. (2005). Co-Occurring Mental and Substance Use Disorders: The Neurobiological Effects of Chronic Stress. *American Journal of Psychiatry*, *162*(8), 1483–1493. https://doi.org/10.1176/appi.ajp.162.8.1483

Calcagnoli, F., de Boer, S. F., Beiderbeck, D. I., Althaus, M., Koolhaas, J. M., & Neumann, I. D. (2014). Local oxytocin expression and oxytocin receptor binding in the male rat brain is associated with aggressiveness. *Behavioural Brain Research*, *261*, 315–322. https://doi.org/10.1016/j.bbr.2013.12.050

Chen, C., Jiang, Z., Fu, X., Yu, D., Huang, H., & Tasker, J. G. (2019). Astrocytes Amplify Neuronal Dendritic Volume Transmission Stimulated by Norepinephrine. *Cell Reports*, *29*(13), 4349-4361.e4. https://doi.org/10.1016/j.celrep.2019.11.092

Chen, S., Xu, H., Dong, S., & Xiao, L. (2022). Morpho-Electric Properties and Diversity of Oxytocin Neurons in Paraventricular Nucleus of Hypothalamus in Female and Male Mice. *The Journal of Neuroscience*, *42*(14), 2885–2904. https://doi.org/10.1523/JNEUROSCI.2494-21.2022

Chini, B., Mouillac, B., Balestre, M.-N., Trumpp-Kallmeyer, S., Hoflack, J., Hibert, M., Andriolo, M., Pupier, S., Jard, S., & Barberis, C. (1996). Two aromatic residues regulate the response of the human oxytocin receptor to the partial agonist arginine vasopressin. *FEBS Letters*, *397*(2–3), 201–206. https://doi.org/10.1016/S0014-5793(96)01135-0

Cornell-Bell, A. H., Finkbeiner, S. M., Cooper, M. S., & Smith, S. J. (1990). Glutamate Induces Calcium Waves in Cultured Astrocytes: Long-Range Glial Signaling. *Science*, *247*(4941), 470–473. https://doi.org/10.1126/science.1967852

Creager, M. A., Faxon, D. P., Cutler, S. S., Kohlmann, O., Ryan, T. J., & Gavras, H. (1986). Contribution of vasopressin to vasoconstriction in patients with congestive heart failure: Comparison with the renin-angiotensin system and the sympathetic nervous system. *Journal of the American College of Cardiology*, *7*(4), 758–765. https://doi.org/10.1016/S0735-1097(86)80333-3

Dabrowska, J., Hazra, R., Ahern, T. H., Guo, J.-D., McDonald, A. J., Mascagni, F., Muller, J. F., Young, L. J., & Rainnie, D. G. (2011). Neuroanatomical evidence for reciprocal regulation of the corticotrophin-releasing factor and oxytocin systems in the hypothalamus and the bed nucleus of the stria terminalis of the rat: Implications for balancing stress and affect. *Psychoneuroendocrinology*, *36*(9), 1312–1326. https://doi.org/10.1016/j.psyneuen.2011.03.003

Dabrowska, J., Hazra, R., Guo, J., DeWitt, S., & Rainnie, D. (2013). Central CRF neurons are not created equal: Phenotypic differences in CRF-containing neurons of the rat paraventricular hypothalamus and the bed nucleus of the stria terminalis. *Frontiers in Neuroscience*, *7*. https://www.frontiersin.org/articles/10.3389/fnins.2013.00156

Dautzenberg, F. M., & Hauger, R. L. (2002). The CRF peptide family and their receptors: Yet more partners discovered. *Trends in Pharmacological Sciences*, *23*(2), 71–77. https://doi.org/10.1016/S0165-6147(02)01946-6

Ebner, K., Bosch, O. J., Krömer, S. A., Singewald, N., & Neumann, I. D. (2005). Release of Oxytocin in the Rat Central Amygdala Modulates Stress-Coping Behavior and the Release of Excitatory Amino Acids. *Neuropsychopharmacology*, *30*(2), 223–230. https://doi.org/10.1038/sj.npp.1300607

Engelmann, Ebner, Landgraf, Holsboer, & Wotjak1. (1999). Emotional Stress Triggers Intrahypothalamic But Not Peripheral Release of Oxytocin in Male Rats. *Journal of Neuroendocrinology*, *11*(11), 867–872. https://doi.org/10.1046/j.1365-2826.1999.00403.x

Erkut, Z. A., Pool, C., & Swaab, D. F. (1998). Glucocorticoids Suppress Corticotropin-Releasing Hormone and Vasopressin Expression in Human Hypothalamic Neurons1. *The Journal of Clinical Endocrinology & Metabolism*, *83*(6), 2066–2073. https://doi.org/10.1210/jcem.83.6.4881

Ganten, D., & Pfaff, D. (Eds.). (1986). *Neurobiology of Oxytocin* (Vol. 6). Springer Berlin Heidelberg. https://doi.org/10.1007/978-3-642-70414-7

Godoy, L. D., Rossignoli, M. T., Delfino-Pereira, P., Garcia-Cairasco, N., & de Lima Umeoka, E. H. (2018). A Comprehensive Overview on Stress Neurobiology: Basic Concepts and Clinical Implications. *Frontiers in Behavioral Neuroscience*, *12*. https://www.frontiersin.org/article/10.3389/fnbeh.2018.00127

Goeij, D. C. E. de, Kvetnansky, R., Whitnall, M. H., Jezova, D., Berkenbosch, F., & Tilders, F. J. H. (1991). Repeated Stress-Induced Activation of Corticotropin-Releasing Factor Neurons Enhances Vasopressin Stores and Colocalization with Corticotropin-Releasing Factor in the Median Eminence of Rats. *Neuroendocrinology*, *53*(2), 150–159. https://doi.org/10.1159/000125712

Grantham, J., & Burg, M. (1966). Effect of vasopressin and cyclic AMP on permeability of isolated collecting tubules. *American Journal of Physiology-Legacy Content*, *211*(1), 255–259. https://doi.org/10.1152/ajplegacy.1966.211.1.255

Grinevich, V., Desarménien, M. G., Chini, B., Tauber, M., & Muscatelli, F. (2015). Ontogenesis of oxytocin pathways in the mammalian brain: Late maturation and psychosocial disorders. *Frontiers in Neuroanatomy*, *8*. https://www.frontiersin.org/articles/10.3389/fnana.2014.00164

Gunaydin, L. A., Grosenick, L., Finkelstein, J. C., Kauvar, I. V., Fenno, L. E., Adhikari, A., Lammel, S., Mirzabekov, J. J., Airan, R. D., Zalocusky, K. A., Tye, K. M., Anikeeva, P., Malenka, R. C., & Deisseroth, K. (2014). Natural Neural Projection Dynamics Underlying Social Behavior. *Cell*, *157*(7), 1535–1551. https://doi.org/10.1016/j.cell.2014.05.017

Guo, Q., Zhou, J., Feng, Q., Lin, R., Gong, H., Luo, Q., Zeng, S., Luo, M., & Fu, L. (2015). Multi-channel fiber photometry for population neuronal activity recording. *Biomedical Optics Express*, *6*(10), 3919–3931. https://doi.org/10.1364/BOE.6.003919

Hamilton, N. B., & Attwell, D. (2010). Do astrocytes really exocytose neurotransmitters? *Nature Reviews Neuroscience*, *11*(4), 227–238. https://doi.org/10.1038/nrn2803

Herman, J. P., Cullinan, W. E., Ziegler, D. R., & Tasker, J. G. (2002). Role of the paraventricular nucleus microenvironment in stress integration*. *European Journal of Neuroscience*, *16*(3), 381–385. https://doi.org/10.1046/j.1460-9568.2002.02133.x

Herman, J. P., McKlveen, J. M., Ghosal, S., Kopp, B., Wulsin, A., Makinson, R., Scheimann, J., & Myers, B. (2016). Regulation of the hypothalamic-pituitary-adrenocortical stress response. *Comprehensive Physiology*, *6*(2), 603–621. https://doi.org/10.1002/cphy.c150015

Herman, J. P., Ostrander, M. M., Mueller, N. K., & Figueiredo, H. (2005). Limbic system mechanisms of stress regulation: Hypothalamo-pituitary-adrenocortical axis. *Progress in Neuro-Psychopharmacology and Biological Psychiatry*, *29*(8), 1201–1213. https://doi.org/10.1016/j.pnpbp.2005.08.006

Hidema, S., Fukuda, T., Hiraoka, Y., Mizukami, H., Hayashi, R., Otsuka, A., Suzuki, S., Miyazaki, S., & Nishimori, K. (2016). Generation of Oxtr cDNAHA-Ires-Cre Mice for Gene Expression in an Oxytocin Receptor Specific Manner. *Journal of Cellular Biochemistry*, *117*(5), 1099–1111. https://doi.org/10.1002/jcb.25393

Holmes, A., Heilig, M., Rupniak, N. M. J., Steckler, T., & Griebel, G. (2003). Neuropeptide systems as novel therapeutic targets for depression and anxiety disorders. *Trends in Pharmacological Sciences*, *24*(11), 580–588. https://doi.org/10.1016/j.tips.2003.09.011

Iwasaki, Y., Kumari, P., Wang, L., Hidema, S., Nishimori, K., & Yada, T. (2019). Relay of peripheral oxytocin to central oxytocin neurons via vagal afferents for regulating feeding. *Biochemical and Biophysical Research Communications*, *519*(3), 553–558. https://doi.org/10.1016/j.bbrc.2019.09.039

Juif, P.-E., Breton, J.-D., Rajalu, M., Charlet, A., Goumon, Y., & Poisbeau, P. (2013). Long-Lasting Spinal Oxytocin Analgesia Is Ensured by the Stimulation of Allopregnanolone Synthesis Which Potentiates GABAA Receptor-Mediated Synaptic Inhibition. *Journal of Neuroscience*, *33*(42), 16617–16626. https://doi.org/10.1523/JNEUROSCI.3084-12.2013

Jurek, B., & Neumann, I. D. (2018). The Oxytocin Receptor: From Intracellular Signaling to Behavior. *Physiological Reviews*, *98*(3), 1805–1908. https://doi.org/10.1152/physrev.00031.2017

Karisetty, B. C., Khandelwal, N., Kumar, A., & Chakravarty, S. (2017). Sex difference in mouse hypothalamic transcriptome profile in stress-induced depression model. *Biochemical and Biophysical Research Communications*, *486*(4), 1122–1128. https://doi.org/10.1016/j.bbrc.2017.04.005

Keverne, E. B., & Curley, J. P. (2004). Vasopressin, oxytocin and social behaviour. *Current Opinion in Neurobiology*, *14*(6), 777–783. https://doi.org/10.1016/j.conb.2004.10.006

Lambert, T. (n.d.-a). *FPbase: The Fluorescent Protein Database*. FPbase. Retrieved August 23, 2022, from https://www.fpbase.org/reference/111/

Lang, R. E., Heil, J. W. E., Ganten, D., Hermann, K., Unger, T., & Rascher, W. (1983). Oxytocin Unlike Vasopressin Is a Stress Hormone in the Rat. *Neuroendocrinology*, *37*(4), 314–316. https://doi.org/10.1159/000123566

Lim, M. M., Wang, Z., Olazábal, D. E., Ren, X., Terwilliger, E. F., & Young, L. J. (2004). Enhanced partner preference in a promiscuous species by manipulating the expression of a single gene. *Nature*, *429*(6993), 754–757. https://doi.org/10.1038/nature02539

Lim, M. M., & Young, L. J. (2004). Vasopressin-dependent neural circuits underlying pair bond formation in the monogamous prairie vole. *Neuroscience*, *125*(1), 35–45. https://doi.org/10.1016/j.neuroscience.2003.12.008

Liposits, Zs., Phelix, C., & Paull, W. K. (1987). Synaptic interaction of serotonergic axons and corticotropin releasing factor (CRF) synthesizing neurons in the hypothalamic paraventricular nucleus of the rat: A light and electron microscopic immunocytochemical study. *Histochemistry*, *86*(6), 541–549. https://doi.org/10.1007/BF00489545

Mack, S. O., Kc, P., Wu, M., Coleman, B. R., Tolentino-Silva, F. P., & Haxhiu, M. A. (2002). Paraventricular oxytocin neurons are involved in neural modulation of breathing. *Journal of Applied Physiology*, *92*(2), 826–834. https://doi.org/10.1152/japplphysiol.00839.2001

McEwen, B. S., & Akil, H. (2020). Revisiting the Stress Concept: Implications for Affective Disorders. *The Journal of Neuroscience*, *40*(1), 12–21. https://doi.org/10.1523/JNEUROSCI.0733-19.2019

Mittaud, P., Labourdette, G., Zingg, H., & Guenot-Di Scala, D. (2002). Neurons modulate oxytocin receptor expression in rat cultured astrocytes: Involvement of TGF-β and membrane components. *Glia*, *37*(2), 169–177. https://doi.org/10.1002/glia.10029

Münch, T. A. (2013). Visual Behavior: Mice Run from Overhead Danger. *Current Biology*, *23*(20), R925–R927. https://doi.org/10.1016/j.cub.2013.08.039

Myers, B., Scheimann, J. R., Franco-Villanueva, A., & Herman, J. P. (2017). Ascending mechanisms of stress integration: Implications for brainstem regulation of neuroendocrine and behavioral stress responses. *Neuroscience & Biobehavioral Reviews*, *74*, 366–375. https://doi.org/10.1016/j.neubiorev.2016.05.011

Nedergaard, M. (1994). Direct Signaling from Astrocytes to Neurons in Cultures of Mammalian Brain Cells. *Science*, *263*(5154), 1768–1771.

Neumann, I. D. (2009). The advantage of social living: Brain neuropeptides mediate the beneficial consequences of sex and motherhood. *Frontiers in Neuroendocrinology*, *30*(4), 483–496. https://doi.org/10.1016/j.yfrne.2009.04.012

Neumann, I. D., & Landgraf, R. (2012). Balance of brain oxytocin and vasopressin: Implications for anxiety, depression, and social behaviors. *Trends in Neurosciences*, *35*(11), 649–659. https://doi.org/10.1016/j.tins.2012.08.004

Nishimori, K., Young, L. J., Guo, Q., Wang, Z., Insel, T. R., & Matzuk, M. M. (1996). Oxytocin is required for nursing but is not essential for parturition or reproductive behavior. *Proceedings of the National Academy of Sciences*, *93*(21), 11699–11704. https://doi.org/10.1073/pnas.93.21.11699

Nishioka, T., Anselmo-Franci, J. A., Li, P., Callahan, M. F., & Morris, M. (1998). Stress increases oxytocin release within the hypothalamic paraventricular nucleus. *Brain Research*, *781*(1), 57–61. https://doi.org/10.1016/S0006-8993(97)01159-1

Ottenweller, J. E., Natelson, B. H., Pitman, D. L., & Drastal, S. D. (1989). Adrenocortical and behavioral responses to repeated stressors: Toward an animal model of chronic stress and stress-related mental illness. *Biological Psychiatry*, *26*(8), 829–841. https://doi.org/10.1016/0006-3223(89)90123-6

Parpura, V., Basarsky, T. A., Liu, F., Jeftinija, K., Jeftinija, S., & Haydon, P. G. (1994). Glutamate-mediated astrocyte–neuron signalling. *Nature*, *369*(6483), 744–747. https://doi.org/10.1038/369744a0

Pati, D., Harden, S. W., Sheng, W., Kelly, K. B., de Kloet, A. D., Krause, E. G., & Frazier, C. J. (2020). Endogenous oxytocin inhibits hypothalamic corticotrophin-releasing hormone neurones following acute hypernatraemia. *Journal of Neuroendocrinology*, *32*(3), e12839. https://doi.org/10.1111/jne.12839

Pati, D., Krause, E. G., & Frazier, C. J. (2022). Intrahypothalamic effects of oxytocin on PVN CRH neurons in response to acute stress. *Current Opinion in Endocrine and Metabolic Research*, 100382. https://doi.org/10.1016/j.coemr.2022.100382

Perkinson, M. R., Kim, J. S., Iremonger, K. J., & Brown, C. H. (2021). Visualising oxytocin neurone activity in vivo: The key to unlocking central regulation of parturition and lactation. *Journal of Neuroendocrinology*, *33*(11), e13012. https://doi.org/10.1111/jne.13012

Peter, J., Burbach, H., Adan, R. A. H., Lolait, S. J., van Leeuwen, F. W., Mezey, E., Palkovits, M., & Barberis, C. (1995). Molecular neurobiology and pharmacology of the Vasopressin/Oxytocin receptor family. *Cellular and Molecular Neurobiology*, *15*(5), 573–595. https://doi.org/10.1007/BF02071318

Plotsky, P. M. (1985). Hypophyseotropic regulation of adenohypophyseal adrenocorticotropin secretion. *Federation Proceedings*, *44*(1 Pt 2), 207–213.

Raggenbass, M. (2001). Vasopressin- and oxytocin-induced activity in the central nervous system: Electrophysiological studies using in-vitro systems. *Progress in Neurobiology*, *64*(3), 307–326. https://doi.org/10.1016/S0301-0082(00)00064-2

Raggenbass, M. (2008). Overview of cellular electrophysiological actions of vasopressin. *European Journal of Pharmacology*, *583*(2), 243–254. https://doi.org/10.1016/j.ejphar.2007.11.074

Rigney, N., Whylings, J., de Vries, G. J., & Petrulis, A. (2021). Sex Differences in the Control of Social Investigation and Anxiety by Vasopressin Cells of the Paraventricular Nucleus of the Hypothalamus. *Neuroendocrinology*, *111*(6), 521–535. https://doi.org/10.1159/000509421

Rivier, C., & Vale, W. (1983). Modulation of stress-induced ACTH release by corticotropin-releasing factor, catecholamines and vasopressin. *Nature*, *305*(5932), 325–327. https://doi.org/10.1038/305325a0

Roland, B. L., & Sawchenko, P. E. (1993). Local origins of some GABAergic projections to the paraventricular and supraoptic nuclei of the hypothalamus in the rat. *Journal of Comparative Neurology*, *332*(1), 123–143. https://doi.org/10.1002/cne.903320109

Rood, B. D., & De Vries, G. J. (2011). Vasopressin innervation of the mouse (Mus musculus) brain and spinal cord. *Journal of Comparative Neurology*, *519*(12), 2434–2474. https://doi.org/10.1002/cne.22635

Ross, H. E., & Young, L. J. (2009). Oxytocin and the neural mechanisms regulating social cognition and affiliative behavior. *Frontiers in Neuroendocrinology*, *30*(4), 534–547. https://doi.org/10.1016/j.yfrne.2009.05.004

Roth, J., Zeisberger, E., Vybíral, S., & Janský, L. (2004). Endogenous antipyretics: Neuropeptides and glucocorticoids. *Frontiers in Bioscience-Landmark*, *9*(1), 816–826. https://doi.org/10.2741/1277

Schrier, R. W. (2006). Water and Sodium Retention in Edematous Disorders: Role of Vasopressin and Aldosterone. *The American Journal of Medicine*, *119*(7), S47–S53. https://doi.org/10.1016/j.amjmed.2006.05.007

Selye, H. (1950). Stress and the General Adaptation Syndrome. *British Medical Journal*, *1*(4667), 1383–1392.

Senst, L., Baimoukhametova, D., Sterley, T.-L., & Bains, J. S. (2016). Sexually dimorphic neuronal responses to social isolation. *ELife*, *5*, e18726. https://doi.org/10.7554/eLife.18726

Shapiro, L. E., & Insel, T. R. (1989). Ontogeny of oxytocin receptors in rat forebrain: A quantitative study. *Synapse*, *4*(3), 259–266. https://doi.org/10.1002/syn.890040312

Simerly, R. B. (1998). Organization and regulation of sexually dimorphic neuroendocrine pathways. *Behavioural Brain Research*, *92*(2), 195–203. https://doi.org/10.1016/S0166-4328(97)00191-5

Smith, A. S., & Wang, Z. (2014). Hypothalamic Oxytocin Mediates Social Buffering of the Stress Response. *Biological Psychiatry*, *76*(4), 281–288. https://doi.org/10.1016/j.biopsych.2013.09.017

Smith, C. J. W., DiBenedictis, B. T., & Veenema, A. H. (2019). Comparing vasopressin and oxytocin fiber and receptor density patterns in the social behavior neural network: Implications for cross-system signaling. *Frontiers in Neuroendocrinology*, *53*, 100737. https://doi.org/10.1016/j.yfrne.2019.02.001

Södersten, P., Henning, M., Melin, P., & Ludin, S. (1983). Vasopressin alters female sexual behaviour by acting on the brain independently of alterations in blood pressure. *Nature*, *301*(5901), 608–610. https://doi.org/10.1038/301608a0

Soloff, M. S., Alexandrova, M., & Fernstrom, M. J. (1979). Oxytocin Receptors: Triggers for Parturition and Lactation? *Science*, *204*(4399), 1313–1315.

Spencer, R. L., & Deak, T. (2017). A users guide to HPA axis research. *Physiology & Behavior*, *178*, 43–65. https://doi.org/10.1016/j.physbeh.2016.11.014

Steinman, M. Q., Duque-Wilckens, N., Greenberg, G. D., Hao, R., Campi, K. L., Laredo, S. A., Laman-Maharg, A., Manning, C. E., Doig, I. E., Lopez, E. M., Walch, K., Bales, K. L., & Trainor, B. C. (2016). Sex-Specific Effects of Stress on Oxytocin Neurons Correspond With Responses to Intranasal Oxytocin. *Biological Psychiatry*, *80*(5), 406–414. https://doi.org/10.1016/j.biopsych.2015.10.007

Sutton, A. K., Pei, H., Burnett, K. H., Myers, M. G., Rhodes, C. J., & Olson, D. P. (2014). Control of Food Intake and Energy Expenditure by Nos1 Neurons of the Paraventricular Hypothalamus. *Journal of Neuroscience*, *34*(46), 15306–15318. https://doi.org/10.1523/JNEUROSCI.0226-14.2014

Swanson, L. W., Sawchenko, P. E., Wiegand, S. J., & Price, J. L. (1980). Separate neurons in the paraventricular nucleus project to the median eminence and to the medulla or spinal cord. *Brain Research*, *198*(1), 190–195. https://doi.org/10.1016/0006-8993(80)90354-6

TAKABATAKE, Y., & SACHS, H. (1964). Vasopressin Biosynthesis. III. In Vitro Studies. *Endocrinology*, *75*(6), 934–942. https://doi.org/10.1210/endo-75-6-934

Tasker, J. G., & Dudek, F. E. (1991). Electrophysiological properties of neurones in the region of the paraventricular nucleus in slices of rat hypothalamus. *The Journal of Physiology*, *434*, 271–293.

The Oxytocin Receptor System: Structure, Function, and Regulation | Physiological Reviews. (n.d.). Retrieved July 4, 2022, from https://journals.physiology.org/doi/full/10.1152/physrev.2001.81.2.629

Vaidyanathan, R., & Hammock, E. A. D. (2017). Oxytocin receptor dynamics in the brain across development and species. *Developmental Neurobiology*, *77*(2), 143–157. https://doi.org/10.1002/dneu.22403

VAN TOL, H. H. M., BOLWERK, E. L. M., LlU, B., & BURBACH, J. P. H. (1988). Oxytocin and Vasopressin Gene Expression in the Hypothalamo-Neurohypophyseal System of the Rat During the Estrous Cycle, Pregnancy, and Lactation. *Endocrinology*, *122*(3), 945–951. https://doi.org/10.1210/endo-122-3-945

VAN TOL, H. H. M., VOORHUIS, D. TH. A. M., & BURBACH, J. P. H. (1987). Oxytocin Gene Expression in Discrete Hypothalamic Magnocellular Cell Groups Is Stimulated by Prolonged Salt Loading. *Endocrinology*, *120*(1), 71–76. https://doi.org/10.1210/endo-120-1-71

Veenema, A. H., Blume, A., Niederle, D., Buwalda, B., & Neumann, I. D. (2006). Effects of early life stress on adult male aggression and hypothalamic vasopressin and serotonin. *European Journal of Neuroscience*, *24*(6), 1711–1720. https://doi.org/10.1111/j.1460-9568.2006.05045.x

Vesuna, S., Kauvar, I. V., Richman, E., Gore, F., Oskotsky, T., Sava-Segal, C., Luo, L., Malenka, R. C., Henderson, J. M., Nuyujukian, P., Parvizi, J., & Deisseroth, K. (2020). Deep posteromedial cortical rhythm in dissociation. *Nature*, *586*(7827), 87–94. https://doi.org/10.1038/s41586-020-2731-9

A- Vigneaud, V. du, Gish, D. T., & Katsoyannis, P. G. (2002, May 1). *A SYNTHETIC PREPARATION POSSESSING BIOLOGICAL PROPERTIES ASSOCIATED WITH ARGININEVASOPRESSIN* (world). ACS Publications; American Chemical Society. https://doi.org/10.1021/ja01647a089

B- Vigneaud, V. du, Ressler, C., Swan, J. M., Roberts, C. W., & Katsoyannis, P. G. (2002, May 1). *The Synthesis of Oxytocin1* (world). ACS Publications; American Chemical Society. https://doi.org/10.1021/ja01641a004

Weber, B., & Barros, L. F. (2015). The Astrocyte: Powerhouse and Recycling Center. *Cold Spring Harbor Perspectives in Biology*, a020396. https://doi.org/10.1101/cshperspect.a020396

Windle, R. J., Shanks, N., Lightman, S. L., & Ingram, C. D. (1997). Central Oxytocin Administration Reduces Stress-Induced Corticosterone Release and Anxiety Behavior in Rats*. *Endocrinology*, *138*(7), 2829–2834. https://doi.org/10.1210/endo.138.7.5255

Wrobel, L. J., Reymond-Marron, I., Dupré, A., & Raggenbass, M. (2010). Oxytocin and vasopressin enhance synaptic transmission in the hypoglossal motor nucleus of young rats by acting on distinct receptor types. *Neuroscience*, *165*(3), 723–735. https://doi.org/10.1016/j.neuroscience.2009.11.001

Wu, Z., Xu, Y., Zhu, Y., Sutton, A. K., Zhao, R., Lowell, B. B., Olson, D. P., & Tong, Q. (2012). An Obligate Role of Oxytocin Neurons in Diet Induced Energy Expenditure. *PLOS ONE*, *7*(9), e45167. https://doi.org/10.1371/journal.pone.0045167

Xiao, L., Priest, M. F., Nasenbeny, J., Lu, T., & Kozorovitskiy, Y. (2017). Biased Oxytocinergic Modulation of Midbrain Dopamine Systems. *Neuron*, *95*(2), 368-384.e5. https://doi.org/10.1016/j.neuron.2017.06.003

Yang, M., & Crawley, J. N. (2009). Simple Behavioral Assessment of Mouse Olfaction. *Current Protocols in Neuroscience*, *48*(1), 8.24.1-8.24.12. https://doi.org/10.1002/0471142301.ns0824s48

Young, L. J., Nilsen, R., Waymire, K. G., MacGregor, G. R., & Insel, T. R. (1999). Increased affiliative response to vasopressin in mice expressing the V1a receptor from a monogamous vole. *Nature*, *400*(6746), 766–768. https://doi.org/10.1038/23475

Young, L. J., & Wang, Z. (2004). The neurobiology of pair bonding. *Nature Neuroscience*, *7*(10), 1048–1054. https://doi.org/10.1038/nn1327

Yu, H., Miao, W., Ji, E., Huang, S., Jin, S., Zhu, X., Liu, M.-Z., Sun, Y.-G., Xu, F., & Yu, X. (2022). Social touch-like tactile stimulation activates a tachykinin 1-oxytocin pathway to promote social interactions. *Neuron*, *110*(6), 1051-1067.e7. https://doi.org/10.1016/j.neuron.2021.12.022

Zelena, D., Pintér, O., Balázsfi, D. G., Langnaese, K., Richter, K., Landgraf, R., Makara, G. B., & Engelmann, M. (2015). Vasopressin signaling at brain level controls stress hormone release: The vasopressin-deficient Brattleboro rat as a model. *Amino Acids*, *47*(11), 2245–2253. https://doi.org/10.1007/s00726-015-2026-x

Zhang, B., Qiu, L., Xiao, W., Ni, H., Chen, L., Wang, F., Mai, W., Wu, J., Bao, A., Hu, H., Gong, H., Duan, S., Li, A., & Gao, Z. (2021). Reconstruction of the Hypothalamo-Neurohypophysial System and Functional Dissection of Magnocellular Oxytocin Neurons in the Brain. *Neuron*, *109*(2), 331-346.e7. https://doi.org/10.1016/j.neuron.2020.10.032

Zhao, L. (2004). Suppression of Proinflammatory Cytokines Interleukin-1 and Tumor Necrosis Factor- in Astrocytes by a V1 Vasopressin Receptor Agonist: A cAMP Response Element-Binding Protein-Dependent Mechanism. *Journal of Neuroscience*, *24*(9), 2226–2235. https://doi.org/10.1523/JNEUROSCI.4922-03.2004

Zingg, H. H., & Laporte, S. A. (2003). The oxytocin receptor. *Trends in Endocrinology & Metabolism*, *14*(5), 222–227. https://doi.org/10.1016/S1043-2760(03)00080-8